https://doi.org/10.5194/acp-2020-128
Preprint. Discussion started: 22 April 2020

Atmospheric Chemistry and Physics Discussions

The trend of the oxidants in boreal forest over 2007-2018: comprehensive modelling study with long-term measurements at SMEAR II, Finland

Dean Chen[1], Putian Zhou[1,2], Tuomo Nieminen[1,3], Pontus Roldin[4], Ximeng Qi[5], Petri Clusius[1], Carlton Xavier[1], Lukas Pichelstorfer[1], Markku Kulmala[1,5], Pekka Rantala[1], Juho Aalto[1], Nina Sarnela[1], Pasi Kolari[1], Petri Keronen[1], Matti P. Rissanen[6], Metin Baykara[1,2], Michael Boy[1,2]

[1]Institute for Atmospheric and Earth Systems Research/Physics, University of Helsinki, P.O. Box 64, 00014 Helsinki, Finland
[2]Climate and Marine Sciences Department, Eurasia Institute of Earth Sciences, Istanbul Technical University, Maslak 34469, Istanbul, Turkey
[3]Institute for Atmospheric and Earth Systems Research/Forest Sciences, University of Helsinki, P.O. Box 64, 00014 Helsinki, Finland
[4]Division of Nuclear Physics, Department of Physics, Lund University, P. O. Box 118SE-221 00 Lund, Sweden
[5]Joint International Research Laboratory of Atmospheric and Earth System Sciences, School of Atmospheric Sciences, Nanjing University, Nanjing, 210023, China
[6]Aerosol Physics Laboratory, Physics Unit, Faculty of Engineering and Natural Sciences, Tampere University, Tampere, Finland

Correspondence to: Putian Zhou (putian.zhou@helsinki.) and Metin Baykara (baykara@itu.edu.tr)

ABSTRACT

Major atmospheric oxidants (OH, O_3 and NO_3) dominate the atmospheric oxidation capacity, while H_2SO_4 is considered as a main driver for new particle formation events. Although numerous studies have investigated the long-term trend of ozone in Europe, the trend of OH, NO_3 and H_2SO_4 at speci c sites are to a large extent unknown. In this study, we investigated how the trends in major atmospheric oxidants (OH, O_3 and NO_3) and H_2SO_4 changed in southern Finland during the past 12 years and discuss how these trends relate to decreasing emissions of regulated air pollutants in Europe.

https://doi.org/10.5194/acp-2020-128
Preprint. Discussion started: 22 April 2020

Atmospheric Chemistry and Physics Discussions

The one-dimensional model SOSAA has been applied in several studies at the SMEAR II station, and has been validated by measurements in several projects. Here, we ran the SOSAA model for the years 2007-2018 to simulate the atmospheric chemical components, especially the atmospheric oxidants and H_2SO_4 at SMEAR II. The simulations were evaluated with observations at SMEAR II for several shorter and longer campaigns. Our results show that OH increased by +1.56 (-0.8; +3.17) % yr^{-1} during daytime and NO_3 decreased by -3.92 (-6.49; -1.79) % yr^{-1} during nighttime, indicating di erent trends of the oxidants during day and night. Sulphuric acid decreased during daytime by -5.12 (-11.39; -0.52) % yr^{-1}, which correlated with the observed decreasing concentration of newly formed particles in the size range 3-25 nm by 1.4% yr^{-1} at SMEAR II during the years 1997-2012 (Nieminen *et al.*, 2014). Additionally we compared our simulated OH, NO_3 and H_2SO_4 concentrations with proxies, which are commonly applied in case limited amount of parameters are measured and no detailed model simulations are available.

1 Introduction

Understanding the atmospheric oxidants (OH, O_3 and NO_3), their reactions and related processes is important as they are the main "cleaning protagonists" of the atmosphere. Many trace gases, such as methane (CH_4), volatile organic compounds (VOCs), nitrogen oxides (NO_x = NO + NO_2) and sulphur dioxide (SO_2) are removed from the atmosphere by oxidation reactions. During the day, the hydroxyl radical (OH) is the dominant oxidant produced by photochemical processes in the troposphere (Gligorovski *et al.*, 2015). Since there is no sunlight at night, the nighttime concentration of OH is signi cantly lower and other oxidants dominate: ozone (O_3) which, during daytime, is formed by OH radical reactions with VOCs in the presence of NO_x, and the nitrate radical (NO_3) which is generated mainly by the reaction of NO_2 with O_3 (Bey *et al.*, 2001; Allen *et al.*, 2002; Brown *et al.*, 2003; Crowley *et al.*, 2010). In general, OH is considered to contribute the most to the atmospheric oxidation capacity (Elshorbany *et al.*, 2009; Volkamer *et al.*, 2010; Mao *et al.*, 2010; Mogensen *et al.*, 2015 Feiner *et al.*, 2016), while O_3 and NO_3 play a minor but nonetheless signi cant role, (Stone *et al.*, 2014). Oxidation of VOCs by OH, O_3 and NO_3 a ect air quality, climate, as well as regional and global budgets of reactive nitrogen, ozone, and secondary organic aerosols (SOA, e.g. Bonn *et al.*, 2004; Claeys *et al.*, 2004; Hallquist *et al.*, 2009; Roldin *et al.*, 2019).

As biogenic sources dominate the global atmospheric VOCs budget (Guenther *et al.*, 1995, 2006), it is important to understand the dynamics of biogenic emissions and their consequences to atmospheric processes. The boreal zone is the world's second largest forested region, after tropical forests (Bonan *et*

https://doi.org/10.5194/acp-2020-128
Preprint. Discussion started: 22 April 2020

Atmospheric Chemistry and Physics Discussions

al., 2008; FAO Global Forest Resources Assessment, 2015) and boreal vegetation is dominated by evergreen coniferous trees that produce signi cant amounts of biogenic VOCs (BVOCs), mainly isoprene (C_5H_8), monoterpenes ($C_{10}H_{16}$) and sesquiterpenes ($C_{15}H_{24}$) (Hakola *et al.*, 1998, 2006; Rinne *et al.*, 2009). Studies of the OH-reactivity in forest canopies have suggested large emissions of unknown reactive BVOCs (Mogensen *et al.*, 2015; Praplan *et al.*, 2019).

Studies on long-term trends of oxidants can provide an insight on how the atmospheric oxidation capacity evolves against the background of climate and local changes in the environment. Several studies have investigated the trends of atmospheric oxidants in Europe. In their studies, Wilson *et al.* (2012) and Yan *et al.* (2018) showed a general decreasing trend in ozone concentrations due to the decrease in NO_x-emissions. Numerous studies have investigated global OH trends using chemical transport models or retrieval of remote sensing of methylchloroform (CH_3CCl_3, MCF) (e.g. Montzka *et al.*, 2000; Prinn *et al.*, 2001, Kirschke *et al.*, 2013). Montzka *et al.* (2011) found a small interannual OH variability, indicating that global OH is generally well bu ered against perturbations. In situ long inter-annual OH measurements are relatively rare. However, one study by Rohrer *et al.* (2006) showed that there was no trend in the level of OH in the Hohenpeissenberg data set during the studied period 1999-2003 (estimate annual trend to be less than ± 2.5% yr^{-1}) and that there was a positive correlation (r=0.941) between OH and the photolysis frequency of ozone, $J(O^1D)$. Long term trends of NO_3 are rarely studied, and only a few modelling studies on the long-term NO_3 trend exist (e.g. Heintz *et al.*, 1996).

A considerable number of eld campaigns, in which OH concentrations were measured, have been compared to the results of modelling simulations (e.g. Eisele and Tanner, 1991; Holland *et al.*, 1995; Petäjä *et al.*, 2009). Most modelling studies reproduced the OH concentration within the uncertainty range of the OH measurements, including clean (e.g. Tan *et al.*, 2001; Ren *et al.*, 2005; Kubistin *et al.*, 2010; Dlugi *et al.*, 2010; Kanaya *et al.*, 2012; Regelin *et al.*, 2013) and urban areas (e.g. Heard *et al.*, 2004; Emmerson *et al.*, 2005; Shirley *et al.*, 2006; Martinez *et al.*, 2007; Emmerson *et al.*, 2007; Gri th *et al.*, 2016). At the Station to Measure Ecosystem - Atmosphere Relation (SMEAR II) (Kulmala *et al.*, 2001), located in Hyytiälä, Finland, OH concentrations were measured in two campaigns: European Integrated project on Aerosol, Cloud, Climate, and Air Quality Interactions (EUCAARI, 2007-2010) (Kulmala *et al.*, 2011) and Hyytiälä United Measurement of Photochemistry and Particles - Comprehensive Organic Particle and Environmental Chemistry (COPECC-HUMPPA) (Williams *et al.*, 2011). Results from these campaigns showed that modelled OH values were slightly overestimated compared to the measured values (Petäjä *et al.*, 2009; Boy *et al.*, 2013). At the

https://doi.org/10.5194/acp-2020-128
Preprint. Discussion started: 22 April 2020

Atmospheric Chemistry and Physics Discussions

COPECC-HUMPPA campaign (Mogensen et al., 2015) and the IBAIRN (In uence of Biosphere-Atmosphere Interactions on the Reactive Nitrogen budget) campaign NO_3 concentrations at SMEAR II were also measured, but most of the time the values were close to the limit of detection (LOD) of the instrument (Liebmann *et al.*, 2018). However, due to the importance of NO_3 radical in oxidation of BVOCs, previous studies developed a NO_3 proxy which can also be used to derive long term trends at the SMEAR II (Kontkanen *et al.*, 2016).

The aim of this study is to provide an insight into the long-term tendency of the atmospheric oxidation capacity at the boreal forest in Finland from 2007 to 2018. Based on this, we estimate how the H_2SO_4 concentration has changed through this period, and how this could a ect the frequency of new particle formation events on this site.

2 Methods

2.1 SMEAR II

The long-term measurements analysed in this study were conducted at SMEAR II station located in Hyytiälä (61°50'51"N, 24°17'41"E), Southern Finland (Hari and Kulmala, 2005). The station is surrounded by 56 years old (in 2018) pine dominated forest, that also contains Norway Spruces and deciduous trees (Bäck *et al.*, 2012). SMEAR II is a unique eld station with continuous measurements of physical, chemical and biological phenomena, processes and interaction between these elements. Detailed description of the site can be found at the SMEAR II website (https://www.atm.helsinki. /SMEAR/index.php/smear-ii).

One of the major changes that a ects the general trend of atmospheric composition is the growing vegetation. The mean height of dominant trees within 200 m from the measurement tower was 16.9 m in the year 2007, and grew to 20.5 m in 2018. The overstory canopy depth was 8 m in the year 2007, and grew to 8.63 m by 2014. Since the year 2014, it stayed constant. The all-sided LAI (Leaf Area Index) of all trees in July grew from 5.5 m^2/m^2 in 2007 to 5.9 m^2/m^2 in 2015. After 2015 it was considered the same as in 2015. The dry biomass of the foliage in the year 2007 was 0.51 kg/m^2, and reached 0.58 kg/m^2 in 2018.

In this study, selected measurements during the period 2007 to 2018 from the SMEAR II station were used as input for the model simulations; partly to nudge the meteorological parameters to the observations (temperature, absolute humidity, wind speed and direction) or as continuous input for selected gases (O_3, NO_x, SO_2, CO and CH_4), solar irradiance (global short wave radiation, photosynthetically active radiation), soil properties (soil temperature, soil water content and soil heat

https://doi.org/10.5194/acp-2020-128
Preprint. Discussion started: 22 April 2020


Atmospheric Chemistry and Physics Discussions

ux) and particle condensation sink (calculated from the particle size distributions which are measured by DMPS and APS). A detailed description for the station instrumentation (parameter, location, time resolution, method, temporal coverage) is available at the SMEAR II website under "List of the measurements" (https://www.atm.helsinki. /SMEAR/index.php/smear-ii/measurements).

Although the SMEAR II started its operational work already in the late 90's, we decided to focus our long-term modelling activities from the year 2007 onwards. The reason was the NO_x monitoring technique and the fact that the NO_x concentrations have large impact on the simulated OH concentrations. Until February 2007, a molybdenum converter was used to convert NO_2 to NO. However, this technique also measures other nitrogen compounds (e.g. nitric acid, nitrous acid, PAN) which are misinterpreted as NO and consequently the NO level is overestimated. Since March 2007, a photolytic Blue Light converter was used for only converting NO_2 to NO, which enables more accurate data of NO (see Fig. S1 in supplementary material).

2.2 SOSAA

SOSAA (a model to Simulate the concentrations of Organic vapours, Sulphuric Acid and Aerosol) is a 1-D chemistry transport model used to study the atmospheric composition inside the planetary boundary layer. In the past, SOSAA been applied to study characteristics of OH-reactivity (Mogensen *et al.*, 2015; Praplan *et al.*, 2019), oxidation of trace gases (Boy *et al.*, 2013), emission of BVOCs (Smolander *et al.*, 2013), vertical exchange and dry deposition of ozone (Zhou *et al.*, 2017a) and BVOCs (Zhou *et al.*, 2017b), respectively, as well as new particle formation and growth of sub-3 nm particles (Zhou *et al.*, 2014). SOSAA is written in Fortran and parallelized with MPI (Message Passing Interface). In this study, four di erent modules were used: 1) the meteorological module, which is derived from SCADIS (Sogachev *et al.*, 2002, 2005; Sogachev and Panferov, 2006); 2) the BVOCs emission module, which is a modi ed version of MEGAN2.04 (Model of Emissions of Gases and Aerosols from Nature; Guenther *et al.*, 2006); 3) the chemistry module, which is created by KPP (Damian *et al.*, 2002), with the chemical mechanism generated by MCM3.3.1 (Jenkin *et al.*, 1997; Saunders *et al.*, 2003; Jenkin *et al.*, 2012; see http://mcm.leeds.ac.uk/ MCM); and 4) the gas dry deposition module, which is modi ed from MLC-CHEM (Ganzeveld *et al.*, 2004; Zhou *et al.*, 2017a and 2017b). SOSAA describes the atmospheric boundary layer evolution and the vertical mixing of the chemical species in 51 vertical layers, from the surface up to 3 km. The simulation time step is 10 s for meteorology module and 60 s for other modules.

https://doi.org/10.5194/acp-2020-128
Preprint. Discussion started: 22 April 2020

Atmospheric Chemistry and Physics Discussions

The meteorological module includes the prognostic equations for horizontal wind vector, air temperature and absolute humidity. In this study, these prognostic variables at the upper boundary of the model domain were constrained with the ERA-Interim reanalysis data which were provided by the European Centre for Medium-Range Weather Forecast (ECMWF) (Dee *et al.*, 2011). In the lower part of the model domain from 4.2 m to 125 m above the ground, the air temperature, wind vector and absolute humidity were nudged to the vertically interpolated measurement data at SMEAR II with a nudging factor of 0.05, which represents the force of regional transport. The incoming short-wave and photosynthetically active radiation (PAR) at the canopy top, as well as the soil properties (soil temperature, soil water content and soil heat ux) were directly read in as input from SMEAR II measurements. The short-wave radiation were provided by the measurement data at SMEAR II, and the radiative transfer module from the ADCHEM model (Roldin *et al.*, 2011) was used to split the observed radiation into the direct and di use, downward and upward radiation components. The radiative transfer module used the quadrature two-stream approximation scheme developed by Toon *et al.* (1989). All of the meteorological input data mentioned above were linearly interpolated to 10 s time resolution to match the simulation time step.

The standard emission potentials of the emitted BVOCs at SMEAR II, which were used to calculate the emission rates, refer to the values suggested in Zhou *et al.* (2017b). The chemistry scheme was derived from the one used in Zhou *et al.* (2017b) but with a newer MCM version 3.3.1. For the reactions of the stabilised Criegee intermediates (sCIs), we diverted from the MCM and instead used newer obtained reaction rates. For the sCIs from α-pinene, β-pinene and limonene, we have used the rates from Mauldin III et al. (2012) similarly to "Scenario C" in Boy et al. (2013). For the sCIs from isoprene, we used the rates from Welz et al. (2012) as done in "Scenario D" in Boy et al. (2013).

The measured mixing ratios of CO, O_3, NO, NO_2 and SO_2 from the height levels 4.2, 8.4, 16.8, 33.6, 50.4, 74.0, 101 and 125 m were vertically averaged and then used as the input values for all the layers in the model. The LOD of SO_2, NO, O_3 and NO_2 were set to 0.06 ppb, 0.05 ppb, 0.3 ppb and 0.1 ppb, respectively (Dr Pasi Kolari, personal discussion). However, for all of these four species there exist several long periods when the measured values went below the LOD. In order to prevent the model from interference of noise, which are too low values, all the values that go below the LOD are set to the LOD. We also did test runs by setting all values below the LOD to LOD/2. However, the model results showed a jump in the simulated OH, NO_3 and H_2SO_4 concentrations at all times the input data went from the LOD to LOD/2. So we decided to use the LOD as a threshold in case the values are below LOD for the four gaseous compounds discussed above. There are several other methods used in

https://doi.org/10.5194/acp-2020-128
Preprint. Discussion started: 22 April 2020


Atmospheric Chemistry and Physics Discussions

the literature to overcome this problem like the "Uniform Fill-In" or the "Log Fill-In" methods discussed and tested by Cohen and Ryan (1998). However, as all data below LOD are unknown no method predicts their distribution correctly which makes it di cult it di cult to choose a single technique that will be best at all times for various parameters. In Table S1 in the supplementary material we calculated the amount of data points for SO_2 and NO above LOD (the two parameters with the highest amount of data below LOD) for di erent percentile ranges in each year to investigate if a trend in the below LOD data exists.

The measured CH_4 concentrations in 2014 were used as input in SOSAA for the year 2014. For other years, an annual growth rate of 6 ppb yr^{-1} was assumed, and the input CH_4 concentrations from 2014 were thus added or subtracted a multiple of the annual growth rate depending on the year di erence. The growth rate were chosen from the 'NASA Earth Observatory' website and represent the methane increase for 2007-2013 (https://earthobservatory.nasa.gov/images/87681/a-global-view-of-methane).

The condensation sinks (CS) for H_2SO_4 and HNO_3 were provided as an input for the model. The CS was calculated based on the particle size distribution measured by a DMPS (particle diameters 3-1000 nm) and an APS (particles with aerodynamic diameters 0.5– 20 m) system (Pirjola *et al.*, 1998; Kulmala *et al.*, 2001), and the hygroscopic growth e ect was corrected based on Laakso *et al.* (2001). Similarly to the meteorological input data, the input mixing ratios and the CS were also linearly interpolated to 60 s time resolution to match the simulation time step of the emission and chemistry modules.

2.3 Statistical methods

The daily/daytime/nighttime trends of variables were calculated based on their daily/daytime/nighttime mean or median values. Whether to use mean or median for a variable is determined by its data value distribution. If the data are logarithmically distributed (O_3, CO, CS, EM-MON, MON, OH, HO_2, H_2SO_4, NO_2, N_2O_5, and NO_3), the median values are used. Here we should notice that although the data value distributions of SO_2 and NO are also logarithmically distributed, we still used their mean values. The reason is that more than 50% of their measured concentrations lie below the LOD, which results in that their median values are equal to LOD. For other variables (temperature, RH, and solar irradiance), the mean values were used. For the logarithmically distributed variables (besides the variables mentioned above, SO_2 and NO are also included here), the daily/daytime/nighttime linear trend ttings were conducted on the logarithm with base 10 of their respective median or mean values.

https://doi.org/10.5194/acp-2020-128
Preprint. Discussion started: 22 April 2020


Atmospheric Chemistry and Physics Discussions

For other variables (temperature, RH, and solar irradiance), the linear trend ttings were performed directly on their respective mean values.

Bootstrapping was used to estimate the con dence interval of the trend (Wilks, D., 1997, Asmi at al., 2013). We rst tted a linear trend to the time series and created a new data set by taking random samples from the original residuals (di erences of the data values and the tted linear trend) and adding these to the linear part. Then a new linear t was made to this new data set. This procedure was repeated several times (typically 1000 iterations). Here the idea was to test the monotonicity of the trend. The smaller the di erences in the tted trends were after many such iterations, the original trend was more likely to be monotonic. To get the con dence interval we examined the 5th to 95th percentile range of the slopes obtained from bootstrapping iterations: if all of the slopes in this range were either positive or negative (thus not containing zero trend), we concluded that the likelihood of there being a trend was higher than 95% ($p<0.05$) and thus statistically signi cant.

To get another estimate of the monotonicity of the trends we also used the Mann-Kendall test for autocorrelated seasonal data (Hipel and McLeod, 1994; Hussain et al., 2019), and the p-values are reported in Table 1 under P_{MK}. The MK test is more conservative, but both our tests agree in the sense that wider con dence interval or larger p-value indicate larger yearly variation and hence the prognostic capacity of the trend is smaller.

Finally, the relative changes (and the 90% con dence interval from the bootstrapping test) which are shown in Table 1 are in linear scale for all variables, describing the actual change in % yr^{-1} or variable units yr^{-1}. The average trendumber eld. You see the Edit Fields dialog. shown in time series plots is obtained with a 1-year running median (window size of ±182 days), see Ma et al.(2016) for a detailed description.

3 Results

The results will be presented in 6 subsections: (1) a short validation of the meteorological module, (2) the trends of measured gases, (3) BVOCs (observation and model inter-comparison), (4) trends and campaign model-observation inter-comparisons for the main oxidants (O_3, OH and NO_3), (5) trends and campaign model-observation inter-comparisons for sulphuric acid and (6) comparisons of proxies for OH, NO_3 and H_2SO_4 with the model results.

Table 1 presents the trends calculated by the method described in subsection 2.3 of both measurements and model output data for certain parameters for the whole day (daily), daytime and nighttime, respectively. The discussion of parameters focuses on the relevant period of daytime (e.g. OH, H_2SO_4, solar irradiance), nighttime (e.g. NO_3) or for the whole day (e.g. O_3, BVOCs). We will focus our

https://doi.org/10.5194/acp-2020-128
Preprint. Discussion started: 22 April 2020


Atmospheric Chemistry and Physics Discussions

discussion on the representative time period. Here the daytime is de ned as the time period between one hour after sunrise and one hour before sunset; nighttime is de ned between one hour after sunset and one hour before sunrise and the daily values are averaged for 24 hours. In the following subsections we will discuss the values for single parameters from Table 1 in more detail.

3.1 Meteorological data analyses

Meteorology is one of the major drivers for the change in atmospheric composition. We compared several measured meteorological parameters with the model outcome to validate the performance of the meteorological module in SOSAA. While temperature, water vapour and wind speed were nudged with the measurements, the heat uxes and net radiation were simulated and their comparison with measurements provide an insight into the simulated energy balance above the forest canopy.

Table 1: Median or mean values, yearly and 12-year trend (in percent or absolute value), P_{MK} values and in brackets the con dence interval of the trend for the yearly change (SWR = short wave irradiance, TEMP = temperature, RH = relative humidity, CS = condensational sink, EM-MON = emission rate for monoterpenes, MON = concentrations of monoterpenes). The rst, second and third rows for each variable except SWR represent daily, daytime and nighttime values, respectively. Modelled results are presented in bold. Detailed description for periods selected (daily, daytime and nighttime) are provided in the text. Statistical methods are explained in subsection 2.3.

https://doi.org/10.5194/acp-2020-128
Preprint. Discussion started: 22 April 2020

Atmospheric Chemistry and Physics Discussions

Parameter	Median (Mean*)	Yearly trend	P_{MK}	12 years trend
SWR*	259.5 [W m^{-2}]	0.62 (-2.54; 1.9) [W m^{-2}]	0.162	7.39 [W m^{-2}]
TEMP*	277.9 [K]	0.07 (0.03; 0.21) [K]	0.769	0.8 [K]
	279.4 [K]	0.07 (0.02; 0.21) [K]	0.740	0.8 [K]
	277.5 [K]	0.07 (-0.02; 0.21) [K]	0.815	0.79 [K]
RH*	80,3 [%]	-0.53 (-1.42; 0.07) [%]	0.215	-6.36 [%]
	77.1 [%]	-0.54 (-1.2; 0.07) [%]	0.206	-6.49 [%]
	81,4 [%]	-0.51 (-1.14; 0.04) [%]	0.233	-6.11 [%]
O_3	7.9E+11 [# cm^{-3}]	-0.11 (-0.86; 0.02) %	0.566	-1.29 %
	8.2E+11 [# cm-^{3}]	-0.17 (-0.83; -0.06) %	0.877	-2.06 %
	7.7E+11 [# cm^{-3}]	-0.03 (-0.89; 0.13) %	0.426	-0.32 %
CO	3.8E+12 [# cm^{-3}]	-0.48 (-1.74; 0.38) %	0.516	-5.64 %
	3.8E+12 [# cm^{-3}]	-0.52 (-1.69; 0.3) %	0.498	-6.01 %
	3.9E+12 [# cm^{-3}]	-0.47 (-1.7; 0.28) %	0.503	-5.51 %
SO_2*	6.6E+9 [# cm^{-3}]	-2.38 (-4.13; -1.18) %	0.012	-25.14 %
	6.5E+9 [# cm^{-3}]	-1.93 (-3.55; -0.83) %	0.022	-20.84 %
	6.5E+9 [# cm^{-3}]	-2.4 (-4.16; -1.19) %	0.013	-25.27 %
CS	4E-3 [s^{-1}]	-1.41 (-4.45; 1.32) %	0.524	-15.71 %
	4E-3 [s^{-1}]	-1.74 (-4.61; 1.2) %	0.440	-18.94 %
	5E-3 [s^{-1}]	-1.25 (-3.8; 1.61) %	0.632	-14.02 %
EM-MON	**1.7E+6 [# cm^{-3}]**	**0.77 (-0.1; 1.88) %**	**0.158**	**9.68 %**
	2.5E+6 [# cm^{-3}]	**0.67 (-0.34; 1.63)**	**0.214**	**8.28 %**
	1.4E+6 [# cm^{-3}]	**0.64 (-0.35; 1.73) %**	**0.197**	**7.97 %**
MON	**4.8E+9 [# cm^{-3}]**	**3.4 (1.23; 6.02) %**	**0.012**	**49.35 %**
	4.6E+9 [# cm^{-3}]	**2.94 (1.05; 5.25) %**	**0.019**	**41.58 %**
	5.3E+9 [# cm^{-3}]	**3.51 (1.43; 6.26) %**	**0.012**	**51.26 %**
OH	**4.7E+5 [# cm^{-3}]**	**2.44 (0.39; 3.89) %**	**0.034**	**33.47 %**
	2.1E+6 [# cm^{-3}]	**1.56 (-0.8; 3.17) %**	**0.104**	**20.41 %**
	2.2E+5 [# cm^{-3}]	**2.79 (0.89; 4.53) %**	**0.032**	**39.06 %**
HO_2	**4.8E+7 [# cm^{-3}]**	**3.57 (1.31; 5.61) %**	**0.013**	**52.37 %**
	1.2E+8 [# cm^{-3}]	**2.89 (0.81; 4.74) %**	**0.041**	**40.56 %**
	3.2E+7 [# cm^{-3}]	**3.66 (1.4; 5.77) %**	**0.012**	**54.01 %**
H_2SO_4	**2.9E+5 [# cm^{-3}]**	**-3.36 (-8.39; 0.84) %**	**0.377**	**-33.67 %**
	1.7E+6 [# cm^{-3}]	**-5.12 (-11.39; -0.52) %**	**0.207**	**-46.74 %**
	1.6E+5 [# cm^{-3}]	**-3.13 (-8.27; 0.6) %**	**0.342**	**-31.71 %**
NO*	2.2E+9 [# cm^{-3}]	-0.04 (-0.33; 0.36) %	0.857	-0.44 %
	4.5E+9 [# cm^{-3}]	-0.23 (-0.75; 0.03) %	0.885	-2.7 %
	1.3E+9 [# cm^{-3}]	0.02 (-0.09; 0.08) %	0.655	0.26 %
NO_2	2.8E+10 [# cm^{-3}]	-3.77 (-6.65; -1.22) %	0.032	-36.92 %
	2.7E+10 [# cm^{-3}]	-3.16 (-5.65; -0.79) %	0.076	-32.00 %
	2.9E+10 [# cm^{-3}]	-3.91 (-6.7; -1.42) %	0.025	-38.02 %
N_2O_5	**1.3E+8 [# cm^{-3}]**	**-8.25 (-13.33; -4.51) %**	**0.013**	**-64.43 %**
	6.9E+7 [# cm^{-3}]	**-6.66 (-11.2; -2.96) %**	**0.017**	**-56.24 %**
	1.8E+8 [# cm^{-3}]	**-8.82 (-14.27; -4.93) %**	**0.010**	**-66.98 %**
NO_3	**4.8E+6 [# cm^{-3}]**	**-3.52 (-5.83; -1.39) %**	**0.011**	**-34.93 %**
	2.8E+6 [# cm^{-3}]	**-2.46 (-4.23; -0.43) %**	**0.028**	**-25.86 %**
	6.2E+6 [# cm^{-3}]	**-3.92 (-6.49; -1.79) %**	**0.009**	**-38.12 %**

274

https://doi.org/10.5194/acp-2020-128
Preprint. Discussion started: 22 April 2020

Atmospheric Chemistry and Physics Discussions

Fig. 1 shows the modelled 12-year median diurnal cycles of sensible and latent heat uxes for the four di erent seasons in 2007-2018. The comparison shows that the modelled values are within 25th - 75th percentiles of the measured ones throughout the whole diurnal cycle in spring and summer, and during 83% time period of the diurnal cycle in autumn. While in winter the model always overestimates the measured sensible heat ux by about 26.2 W m^{-2} in average. During spring, the modelled latent heat ux is about 18.4 W m^{-2} lower compared to the observations, which could be related to the melting of the snow cover on the ground. Note that snow cover is not explicitly modelled in SOSAA. However, during summer, model and measurement show good agreement. For the winter and autumn months, the simulated latent heat ux presents the similar overestimation as the sensible heat ux. In autumn, only 37.5% of the modelled latent heat ux are within the 25th – 75th percentile range. For the other seasons they are most of the time within this range. We want to point out that the measured uxes in the winter and autumn months are very low (< 10 W m^{-2}) and an overall underestimation of heat uxes is normal when applying the eddy covariance technique (Foken, T., 2008) like at SMEAR II; hence making it di cult to form a conclusion on the accuracy of either the model or measurement during these periods.

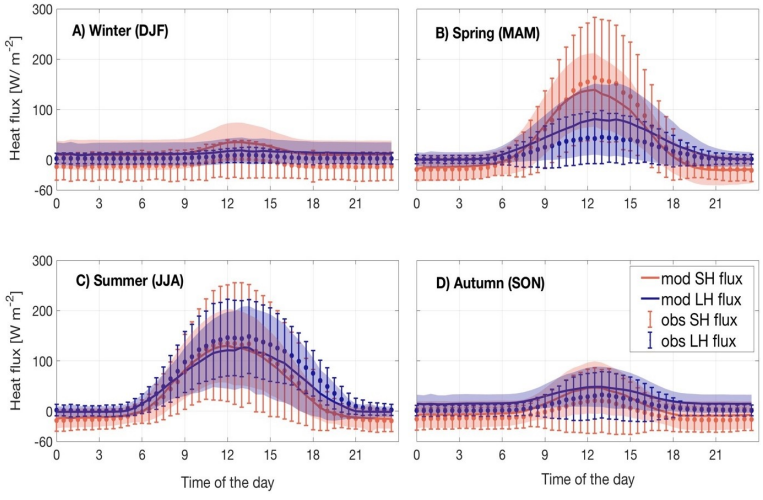

Figure 1: Measured (obs, dots) and modelled (mod, solid lines) diurnal median sensible (SH, red) and Latent (LH, blue) heat uxes above the SMEAR II station (23 m) averaged for the four seasons over the period 2007-2018 in subplots A-D. The letters in brackets in the subplot titles represent the months used for the individual seasons. The 25th – 75th percentile is shown as shades and vertical bars for modelled and measured uxes, respectively.

https://doi.org/10.5194/acp-2020-128
Preprint. Discussion started: 22 April 2020

Atmospheric Chemistry and Physics Discussions

296

297 Fig. 2 shows the observed and simulated averaged diurnal cycle of net radiation at 125 m for each
298 month in the period 2007-2018. Here, the net radiation is calculated as the total incoming short- and
299 long-wave radiation subtracting the total outgoing short and long-wave radiation at the canopy top.
300 Thus positive values represent more incoming than outgoing radiation and vice versa. The modelled
301 daytime values agree well with the measurements in autumn (September, October and November) and
302 early winter (December and January), while the model overestimates the measurements from late
303 winter (February) through summer, with the exception of July. The overestimation occurs mostly at
304 noon with the averaged noon peak overestimated values ranging from ~20 Wm^{-2} to ~100 Wm^{-2}. By
305 contrast, the modelled nighttime net radiation underestimated the measurements by about ~10 Wm^{-2} to
306 ~50 Wm^{-2} on average from September to December and from January to March. In general, the model
307 is consistent with the measurements, and is able to capture the diurnal pattern and seasonal trend of net
308 radiation above the canopy. Therefore, considering the simulation results of SH and LH discussed
309 above, the model can predict a reasonable energy balance inside and above the canopy.

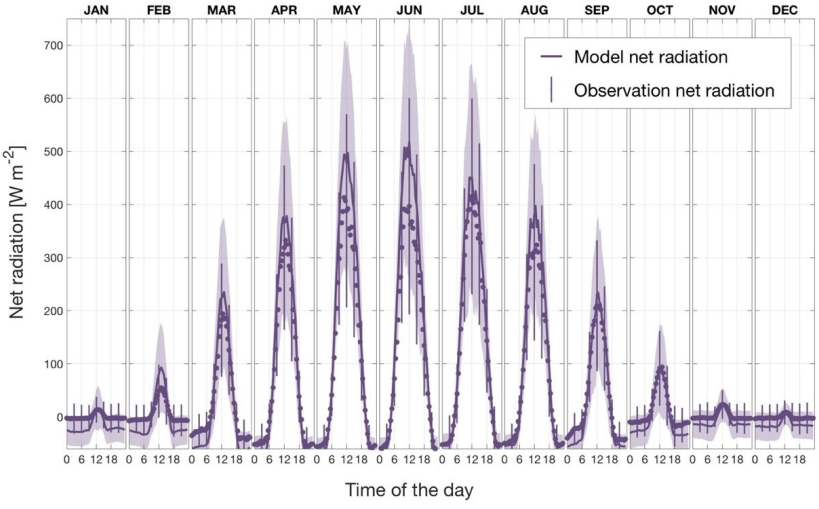

310

311 *Figure 2: Observed and simulated averaged diurnal cycles of net radiation at SMEAR II for each*
312 *month separately for the years 2007-2018.*

313

314 In Table 1, the temperature and relative humidity represent the analyses of the measured data which are
315 used to nudge the model as mentioned above. The trend for daily mean temperature shows an increase
316 of +0.07 (+0.03; +0.21) K yr^{-1} for 2007-2018, which adds up to 0.8 K over the 12 years. This observed

https://doi.org/10.5194/acp-2020-128
Preprint. Discussion started: 22 April 2020


Atmospheric Chemistry and Physics Discussions

warming is in good agreement with earlier studies (Zhang *et al.*, 2019, Räisänen, 2019). The relative humidity shows an opposite behaviour for the same time and decreased at the SMEAR II station by -0.54 (-1.42; +0.07) % yr^{-1} during the period 2007-2018. The reasons for this drop of RH could be various. However, since the trend is not statistically signi cant, the result can be attributed to large interannual variation. Similar to RH the daily downward shortwave radiation increase by +0.62 (-2.54; +1.9) Wm^{-2} yr^{-1} is statistically not signi cant. A gure showing the 12 years daily values and the trends of the above discussed parameters is presented in the supplementary material (Fig. S2).

3.2 Trend of inorganic gases and CS

The main inorganic gases (CO, O_3, NO, NO_2 and SO_2) that are read in as input to SOSAA re ect the in uence of human impact on a regional scale. Carbon monoxide for example has a lifetime of approximately 1-3 months (Seinfeld and Pandis, 2006), and the concentration levels reveal the impact of large regional to hemispherical features. Nitrogen oxides and sulphur dioxide have lifetimes of days to weeks, respectively, and they are mainly related to local or regional changes. At a clean background station like SMEAR II, their concentrations are often below the LOD of the instruments.

The 12-years concentrations of ve measured trace gases (CO, O_3, NO, NO_2 and SO_2) and the aerosol condensation sink (see Table 1 and Fig. S2 in supplementary material) all show a negative trend re ecting the decreased anthropogenic impact on these gases in Europe during the last decades (Hoesly *et al.*, 2018). This trend for Europe was also con rmed by the latest EAA report (No 12/2018). Our trend analyses of daily values show that NO and O_3 concentrations only have a marginal decrease of -0.04 (-0.33; +0.36) % yr^{-1} and -0.11 (-0.86; +0.02) % yr^{-1}, respectively, while the concentrations of CO, SO_2 and NO_2 drop by -0.48 (-1.74; +0.38) % yr^{-1}, -2.38 (-4.13, +1.18) % yr^{-1} and -3.77 (-6.65; -1.22) % yr^{-1}, respectively. We should notice that among these ve compounds, only SO_2 and NO_2 show a signi cant trend as the con dence intervals for the other three gases are both positive and negative and the P_{MK} values are greater than 0.4.

However, as pointed out in subsection 2.3, more than half of the SO_2 and NO measurements are below the LOD of the instruments. Table S1 (in supplementary material) shows the fraction of the NO and SO_2 measurements being below the LOD in a year-wise fashion. There is a clear increase from 2007 to 2018 for SO_2 which points to a stronger decrease than the 2.38% per year mentioned above. For NO, the amount of data measured below LOD are much higher. Note that in the evolutions of the mean values and the 90^{th} and 75^{th} percentile for NO, no trend is observed concerning the quantity of days below LOD (see also discussion in subsection 2.3). Further, there is a decrease in the condensation

https://doi.org/10.5194/acp-2020-128
Preprint. Discussion started: 22 April 2020

Atmospheric Chemistry and Physics Discussions

sink by +1.41 (-4.45; +1.32) % yr^{-1}, partly related to the reduction of primary aerosol emissions from tra c, industry and heating (Nieminen *et al.*, 2014). However, this decreasing trend is not statistically signi cant.

3.3 BVOC'S COMPARISONS AND TRENDS

3.3.1 VALIDATION OF MONOTERPENE MODEL RESULTS

At SMEAR II, monoterpenes are the dominant BVOCs (Bäck *et al.*, 2012), and they are the major contributors to the OH reactivity of the measured organic compounds (Mogensen *et al.*, 2015; Praplan *et al.*, 2019). Thus, accurate modelling of monoterpenes is a crucial component for calculating the OH concentration. Furthermore, the monoterpenes (at SMEAR II) are climatically important because they can be oxidized to form low volatile organic compounds (LVOCs) and hence contribute to secondary aerosol formation (Roldin *et al.*, 2019). Anthropogenic volatile organic compounds (AVOCs) are not included in this study but their concentrations at the SMEAR II are small compared to BVOCs (Hellén *et al.*, 2018).

Fig. 3 shows the modelled versus the measured monoterpene concentrations between 0 m and 150 m at SMEAR II. Both the measurements and the simulations of monoterpene concentrations, show an increase in canopy and decline above the canopy. However, the peak from the measurements is at 8.4 m, while the model show the highest values at 16.8 m. Modelled and measured values decrease at a similar rate above the canopy. The model results at 4.2 m and 8.4 m are lower than the measurements, while at 16.8 m, the model overestimates the concentrations. The di erent height level of the maximum could be related to the distribution of the emission inside the model (MEGAN) but also due to the in uence by micrometeorology (since small bias in the turbulence could have a big in uence). Another reason for the underestimation of the measured concentrations in the lower part of the canopy could be related to the emission of monoterpenes from ground vegetation and soil as reported by Aaltonen *et al.* (2011). Currently, these sources of terpenes are not included in SOSAA and may explain the discrepancy in the lower canopy. For this reason, we compared the measured and modelled monoterpenes concentrations for heights above the canopy (20-120m).

https://doi.org/10.5194/acp-2020-128
Preprint. Discussion started: 22 April 2020

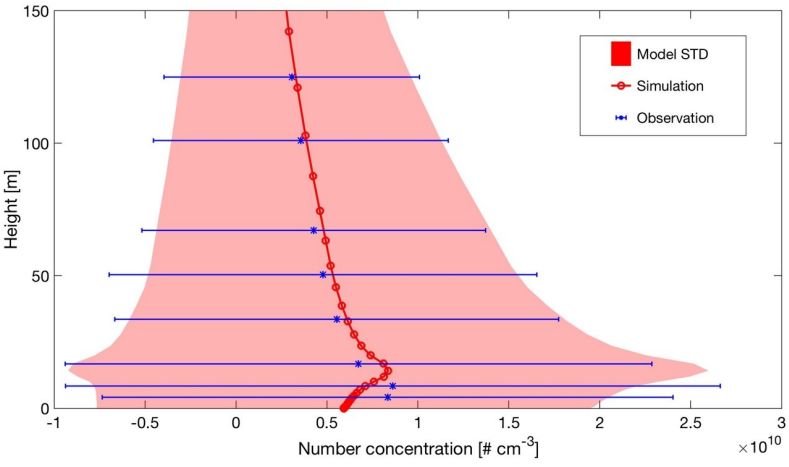

Figure 3: Vertical pro les of measured and modelled monoterpene mean concentrations and ±1 standard deviation at SMEAR II, Finland for the years 2007-2014 and 2017-2018 (2015-2016 measurement data were not available).

In Fig. 4 we compared the measured monoterpene concentrations against the model outcome between 20 m and 40 m for all years except years 2015 and 2016 (measured data were not available for this period). The model slightly underestimates the monoterpene concentrations in winter while overestimating the values in summer. In years when the summer was exceptionally warm (e.g. 2018), the model overestimated the monoterpenes concentration by a factor of 2-3. The reason for this overshooting of the model during hot summers could be that the decrease of monoterpene emissions in the forest through drought is not accurate represented in the emission module MEGAN. In general, 29 % of the time the modelled concentrations are within the range of 25th and 75th percentile of the measured data points.

https://doi.org/10.5194/acp-2020-128
Preprint. Discussion started: 22 April 2020

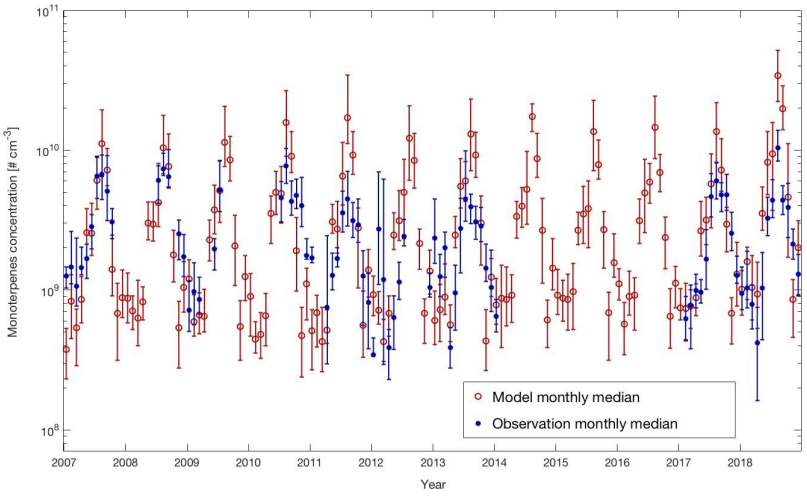

Figure 4: Measured and modelled monthly median values of monoterpene concentrations from 2007 to 2018 for the height interval 20 m-40 m. The 25th and 75th percentile for both data sets are shown as vertical bars.

Although the SMEAR II station is surrounded by a homogeneous pine forest, the distribution of the biomass inside the forest and the vertical mixing lead to inhomogeneity of terpene distribution and point measurement of concentrations at one height level might not be representative. Therefore, we compared the model results with monoterpene ux measurements, which can represent the exchange of the BVOCs over a footprint area (see Fig. S3 in supplementary material). The monoterpenes' uxes data were available only for the years 2010-2013, and comparison between modelled and measured uxes show that they resemble each other. The trend is very similar and 46.1 % of the time the modelled values are in the range of the 25th and 75th percentile of the measurements.

3.3.2 Long term time series of monoterpenes

Previous studies used the empirical proxies method to investigate monoterpene seasonal and diurnal variations (Kontkanen *et al.*, 2016), which may contain high uncertainties. Based on the long-term and evaluated simulations of monoterpenes concentrations by SOSAA, we analysed the long-term trend of monoterpenes concentrations at SMEAR II and presented the results in Table 1. The results show that annual mean daily emissions and concentrations of monoterpenes increased during the last 12 years by

https://doi.org/10.5194/acp-2020-128
Preprint. Discussion started: 22 April 2020


Atmospheric Chemistry and Physics Discussions

410 +0.77 (-0.1; +1.88) % yr^{-1} and +3.4 (+1.23; +6.02) % yr^{-1}, respectively. This can partly be explained by
411 the growing canopy depth and dry weight of biomass (see subsection 2.1).
412
413 3.4 Long term trends of the oxidants
414 3.4.1 Ozone – O_3
415 Ozone is one of the most important oxidants in the atmosphere and thereby its trend during 2007-2018
416 will be discussed here based on the continuous measurements at SMEAR II. Fig. S2b and Table 1
417 show that the ozone concentrations are relative stable over the 12 years (change is -0.11 (-0.86; +0.02)
418 % yr^{-1}). While there is a weak decrease of O_3 during daytime (-0.17 (-0.83; -0.06) % yr^{-1}), the
419 nighttime concentration is stable (change is -0.03 (-0.89; +0.13) % yr^{-1}). Even though NO_x, which is
420 one important parameter for the chemical production of ozone in the lower troposphere through VOCs,
421 decreases substantially during the same time, the decrease of ozone is negligible. A number of studies
422 have shown that in rural areas where NO_x concentrations decrease (e.g. Ordenez *et al.*, 2007; Boleti *et*
423 *al.*, 2018), there are some areas where the ozone concentration shows inevident change or slight
424 decrease.
425
426 3.4.2 Hydroxyl radical - OH
427 The hydroxyl radical, OH is the most important oxidant in the troposphere and it is the major "cleaning
428 protagonist" in the atmosphere by reacting with nearly all trace gases including the vast number of
429 VOCs emitted from the boreal forest. OH is also the most important sink term for methane (CH_4), the
430 second most important greenhouse gas, responsible for approximately 20 % of induced global radiative
431 forcing since pre-industrial times (Turner *et al.*, 2018). OH is also crucial for the sulphuric acid
432 production and in this way, it indirectly in uences the formation of secondary organic aerosols (see
433 subsection 3.5). Therefore, it is important to study the trend of the OH concentrations and to
434 investigate whether increased temperature or changes in the gas-phase composition in the atmosphere
435 during the last decade at the SMEAR II station had an impact on the OH concentrations.
436 The OH measurements are di cult and expensive and therefore measurements of OH at the SMEAR II
437 are rare. In this study, the measurements from the EUCAARI 2007 (Kulmala *et al.*, 2011) and the
438 COPECC-HUMPPA in 2010 (Williams *et al.*, 2011) campaigns were used to evaluate the model
439 performance. To test the simulated OH concentration, we compared measured data from these two
440 campaigns against the model results (Fig. 5). Fig. S4 in supplementary material presents the scatter

https://doi.org/10.5194/acp-2020-128
Preprint. Discussion started: 22 April 2020

Atmospheric Chemistry and Physics Discussions

plots and the daily patterns of both campaigns. Detailed descriptions of the instruments applied for the OH measurements are provided in Kulmala *et al.* (2011) and Williams *et al.* (2011).

During the campaign in 2007, the model overpredicted the OH concentrations substantially but the model performance show better agreement in 2010. The main cause for the discrepancies between the two measured data sets is related to the two di erent seasons (May and August) the campaigns were conducted. The reason why the model agrees well with the measurements in August and rather poorly in May is more complex. Additional studies comparing measured and modelled OH-reactivity at the same location (Mogensen *et al.* 2011 and 2015; Arnaud *et al.*, 2019) showed a high missing OH-reactivity while including all measured gaseous compounds in SOSAA. These discrepancies indicate the existence of unknown compounds during springtime and early summer, which are not included in SOSAA. Preferred reaction of those species with the hydroxyl radical might explain the simulated, strong overestimation of the OH concentration at the SMEAR II. Note that the uncertainty of point measurements is considerable for the boreal forest environment as already mentioned in subsection 3.3.1. The overall conclusion is that SOSAA is able to simulate the OH concentrations at SMEAR II in a su cient way during summer but overestimates OH in spring. There are no measurements for other seasons available for comparison.

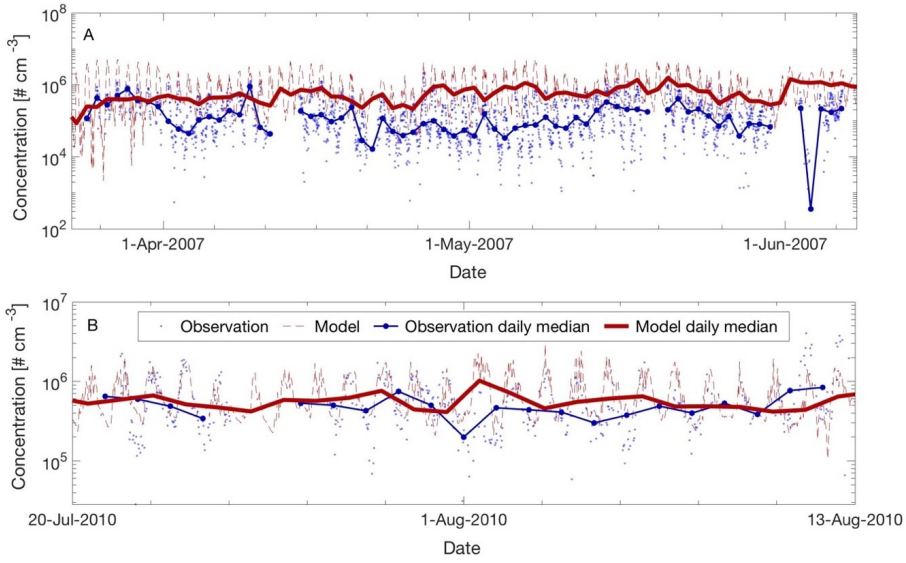

Figure 5: Measured versus modelled hydroxyl radial concentrations for two periods during the EURCAARI (A) and the COPPEC-HUMPPA (B) campaigns.

https://doi.org/10.5194/acp-2020-128
Preprint. Discussion started: 22 April 2020

Atmospheric Chemistry and Physics Discussions

Fig. 6 provides the time-series of modelled OH concentrations from 2007 to 2018. The concentration of OH increased by +1.56 (-0.8; +3.17) % yr^{-1} during daytime and +2.79 (+0.89; +4.53) % yr^{-1} at nighttime. The concentration shows a clear seasonal cycle with peaks in spring and late summer, which partly result from the patterns of ozone (peak in spring, see Fig. S2) and the solar irradiance (peak in summer, see Fig. S2), both required to produce excited oxygen atoms ($O(^1D)$). As the daytime OH concentration is the most important compound for the oxidation capacity of the atmosphere (Mogensen *et al.*, 2015), we only show the daytime mean OH concentration in Fig. 6.

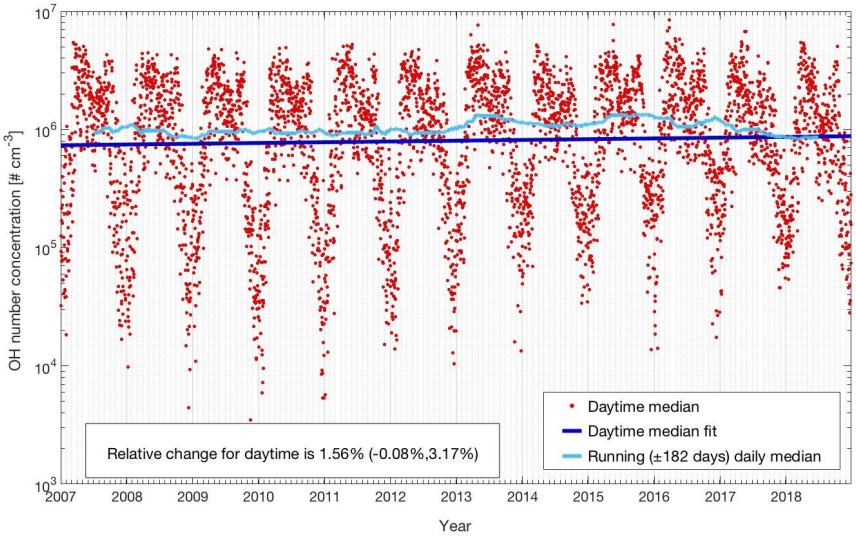

Figure 6: Modelled OH concentrations for the years 2007 to 2018 at the SMEAR II station. Plotted are the daytime median values and the trends calculated with the linear t and running median method which are described in detail in subsection 2.3.

The increasing trend of the OH concentrations at the SMEAR II station is somehow surprising on the rst view, considering the increase of the monoterpene concentrations for the same period. Besides reacting with OH and being a sink term for OH, monoterpenes also produce OH through reaction with ozone. This is the main source of OH during dark conditions at SMEAR II and the nighttime increase of the hydroxyl radical by about 2.8% yr^{-1} is related to this mechanism. However, the absolute OH nighttime concentrations are less than one tenth of the daytime values and therefore the ozonolysis of monoterpenes has only a small contribution to the daytime increase of OH in our calculations. As pointed out in earlier publications (e.g. Boy *et al.*, 2006; Praplan *et al.*, 2019), carbon monoxide (CO) is the main sink term for OH and accounts for about 40% of the removal of OH in the troposphere. CO

https://doi.org/10.5194/acp-2020-128
Preprint. Discussion started: 22 April 2020

Atmospheric Chemistry and Physics Discussions

has a lifetime of 1-3 months (Seinfeld and Pandis, 2006) and has decreased since the 1990s, as shown by Greenland rn air records (Wang *et al.*, 2012; Petrenko *et al.*, 2013) and by surface ask samples collected at few sites (Khalil and Rasmussen, 1994; Novelli *et al.*, 2003; Gratz *et al.*, 2015; Schultz *et al.*, 2015). The drop of CO in our study (0.5% yr^{-1}) a ects the OH trend more than the increase of BVOCs as other important parameters concerning the OH production (e.g. solar irradiance or ozone concentrations) are more or less unchanged during the 12 years. Additionally, the hydroperoxyl radical (HO_2) surprisingly indicates a positive trend of +2.89 (+0.81; +4.74) % yr^{-1}, even stronger compared to OH. This is related to the decrease of the NO concentrations as the nitrogen monoxide is by far the most important sink term for HO_2 (Boy *et al.*, 2006).

3.4.3 Nitrate radical – NO_3

The nitrate radical simulated in this study can't be validated by observations, due to lack of measurements at the SMEAR II. However, by constraining SOSAA with accurately measured NO_2 concentrations, we assume that the predicted NO_3 concentrations are reasonable. The rapid photolysis of NO_3 and the reaction with NO typically reduces its lifetime to a few minutes during daytime. The main contribution of the nitrate radical to the oxidation capacity of the atmosphere is during nighttime. Based on this, we will focus our analysis on the nighttime period.

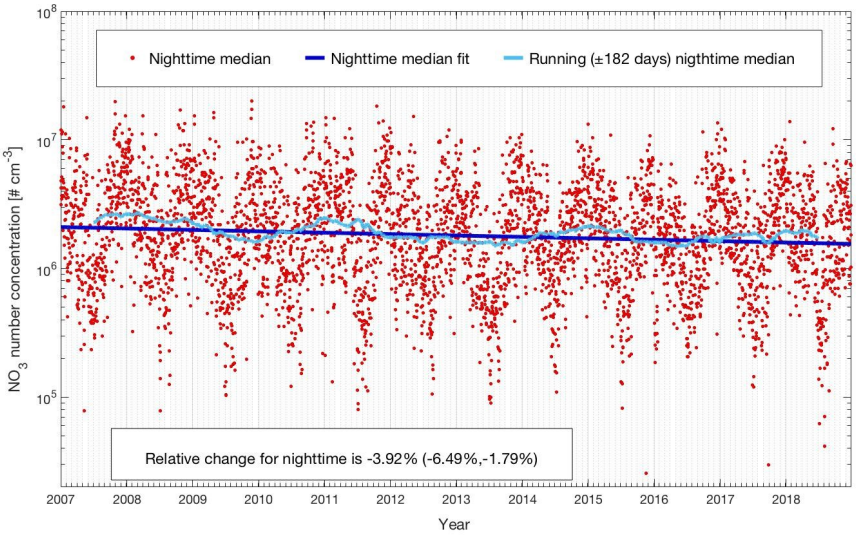

Figure 7: Modelled NO_3 concentrations for the years 2007 to 2018 at the SMEAR II station. Presented are the nighttime median values and the trends calculated with the linear t and running median which are described in detail in subsection 2.3.

https://doi.org/10.5194/acp-2020-128
Preprint. Discussion started: 22 April 2020


Atmospheric Chemistry and Physics Discussions

503

504 Fig. 7 presents the nighttime median NO_3 concentration and the trends for the selected 12 years. The
505 seasonal cycle shows a double-peak in late autumn and early spring, respectively. The reason is that the
506 NO_2 concentration is highest during these periods (see SF2 in supplementary material). As for the
507 trend, the daytime and nighttime inter-annual trends are quite alike. The decreasing trend at night-time
508 (-3.92 (-6.49; -1.79) % yr^{-1}) is slightly higher than the decreasing trend at daytime (-2.46% yr^{-1}). The
509 running median also shows an oscillation of 3-3.5 years during the years 2007-2018, but since this
510 period is relatively short, it is hard to conclude on the reasons.

511

512 ### 3.5 Sulphuric acid model comparison and long-term trends

513 According to the latest global chemistry-transport model simulations, which used state-of-the-art new
514 particle formation (NPF) parameterizations from the CLOUD chamber experiments in CERN (Kirkby
515 *et al.*, 2016; Riccobono *et al.*, 2014), present daytime NPF can almost exclusively be explained by
516 H_2SO_4 clustering with either ammonia or organic compounds formed from OH-oxidation of
517 monoterpenes (Dunne *et al.*, 2016; Gordon *et al.*, 2017). Roldin *et al.* (2019) very recently reproduced
518 observed NPF by considering sulphuric acid together with ammonia and/or ELVOCs during two
519 periods in spring 2013 and 2014. Hence it is crucial for all NPF analyses to know the concentrations of
520 H_2SO_4 and how they have changed in the past and will change in the future.
521 Sulphuric acid was measured at SMEAR II during the last years for several periods. In Fig. 8, we
522 provide a comparison with the outcome of our model simulations for the years 2016 to 2018 (scatter
523 plot and daily distributions for these data sets are provided in SF5 in supplementary material). A
524 detailed description of the instrument used in this study to measure sulphuric acid at the SMEAR II is
525 provided in Jokinen *et al.* (2012).

https://doi.org/10.5194/acp-2020-128
Preprint. Discussion started: 22 April 2020

Atmospheric Chemistry and Physics Discussions

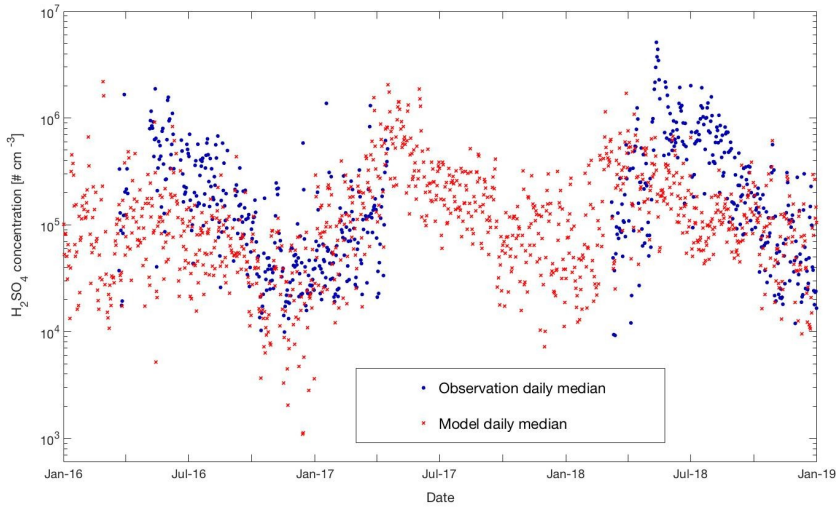

Figure 8: Measured and modelled daily median sulphuric acid concentrations at SMEAR II for the years 2016-2018.

During most of the daytime in spring and summer, the model tends to underestimate the measured concentrations but shows a very good agreement for the same time of the day during autumn and winter. At winter nighttime, the observations are partly below the model results and reach values down to a couple of hundreds of molecules per cm^3. However, the LOD of the instrument is 4E4 molecules cm^{-3} (Jokinen *et al.*, 2012) and most of the measurements during that period are below the LOD. Both the model and the observations present an interesting pattern for the three years: a peak in early spring and then a continuous decline of concentrations for the rest of the year. There is a smaller second peak in summers visible in the model data set, but these peaks are weaker compared to the spring peaks as can be also seen in Fig. 9, which provides the modelled 12 years daytime median concentrations of sulphuric acid.

https://doi.org/10.5194/acp-2020-128
Preprint. Discussion started: 22 April 2020

Atmospheric Chemistry and Physics Discussions

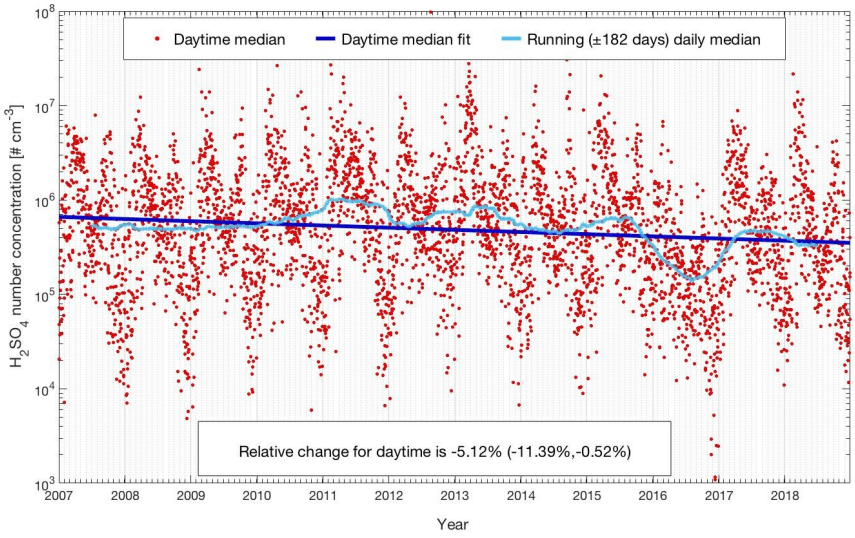

Figure 9: Modelled sulphuric acid concentrations for the years 2007 to 2018 at the SMEAR II station. Shown are the daytime median values and the trends calculated the linear fit and running median which are described in detail in subsection 2.3.

The reason for this pattern which is visible in the model outcomes for all years is a combination of mainly three effects: SO_2, one of the two main precursors for H_2SO_4, is peaking in late winter and early spring and OH reaches its yearly maxima in spring. Additionally, the condensation sink, representing the rate of how fast sulphuric acid molecules will condense on the existing particles, has a clear maxima in summer (SF2 in supplementary material). These three parameters are mainly responsible for the sulphuric acid pattern. Note that a similar pattern has been observed for the occurrence of NPF events at the SMEAR II for several years (Nieminen *et al.*, 2014).

Nieminen at al. (2014) predicted the trend of sulphuric acid based on a proxy calculation (see next subsection) with -1.3% on NPF days and -0.3% on non-NPF days per year for the years 1997-2012. In our study, we applied SOSAA simulations for the years 2007-2018 for the same location. Our model results predict a stronger decrease of daytime H_2SO_4 of -5.12 (-11.39; -0.52) % yr^{-1} (see Table 1). However, the confidence interval of this trend is quite broad, which tells that caution should be taken to interpret this trend too far to the future. The trend in the studied time span is greatly influenced by the large yearly variation, especially year 2016 deviates, which can be seen in Fig. 9. However, this strong drop for 2016 is not visible in the OH concentration but is more related to relatively low values of SO_2 during this year (especially during the summer months). Although the CS values during the first half of

https://doi.org/10.5194/acp-2020-128
Preprint. Discussion started: 22 April 2020

Atmospheric Chemistry and Physics Discussions

this year are low compared to other years and thus would point to even higher sulphuric acid concentrations, the very low sulphur dioxide concentrations seems to have a stronger impact on the H_2SO_4.

3.6 Proxy comparison for OH, H_2SO_4 and NO_3

During the last years, several proxies have been developed for compounds like the hydroxyl or the nitrate radical, due to absence or sparse long-time observations for these parameters. In this subsection, we will compare some of these proxies with the outcome of our model simulations for SMEAR II. This, however, should not be seen as a validation of the proxy but rather to investigate how well simulations agree with them. The proxies compared were developed based on datasets from the SMEAR II.

The first proxy we compare is for the OH radical. It is based on a publication by Nieminen at al. (2014). The results of the proxy, together with the outcome of the model simulations, are presented in Fig. 10. In this proxy, the hydroxyl radical is calculated as;

$$[OH] = ((8.4 * 10^{-7} / 8.6 * 10^{-10}) * UVB^{0.32})^{1.92} \quad \text{Eq. 1}$$

Here *UVB* presents the ultraviolet irradiance measured at SMEAR II. The modelled and the proxy OH concentrations show a similar trend from October to April but start to diverge from May to September with the highest discrepancy around late May to late June. During this time the modelled OH concentrations are about two-fold higher compared to the proxy. Later in the year from July to September the modelled values are still higher compared to the proxy but the discrepancy decreases.

As pointed out in subsection 3.4.2, we believe, based on OH-reactivity measurements at SMEAR II, there exist missing compounds reacting with OH. Taking this into account and assuming that the missing compounds originate from the local ecosystem with maximum emissions during the most biologically active period, the modelled OH concentrations are potentially too high during spring and summer and the proxy would be more accurate at these times. However, as long as these unknown compounds are not identified and no long-term measurements of OH at the SMEAR II exist, any final conclusion about whether the proxy or the model is more correct can only be speculation.

https://doi.org/10.5194/acp-2020-128
Preprint. Discussion started: 22 April 2020

Atmospheric Chemistry and Physics Discussions

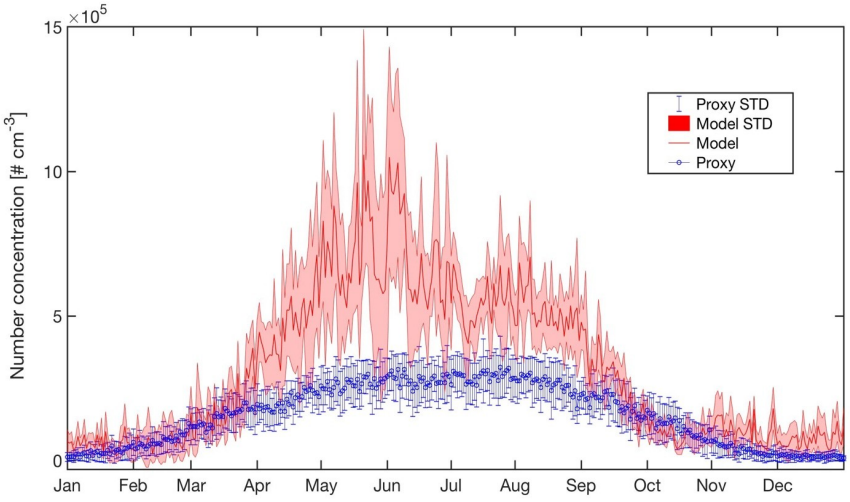

Figure 10: Yearly mean daily time series of OH concentrations estimated by SOSAA (Model) and a proxy parameterisation (Proxy) for the year 2007-2018 at SMEAR II. Details for the applied proxy are provided in the text.

The next proxy we compare with our model simulations is for sulphuric acid. It is based on a parameterization method from Petäjä *et al.* (2009). The proxy is calculated as follows,

$$[H2SO4] = k * [SO2] * UVB / CS \quad \text{Eq. 2}$$

Here *UVB* stands for the ultraviolet irradiance, *CS* for the condensational sink and $[SO_2]$ for the gas phase concentration of sulphur dioxide. The scaling factor k is an empirically derived factor, which scales the proxy variables to correspond to the measured sulphuric acid concentrations. As already pointed out in the previous subsection, the modelled sulphuric acid concentrations show a clear peak in early spring and then a nearly continuous decrease for the rest of the year (see Fig. 11). The proxy follows this pattern almost identically from April to September but exceeds the modelled data approximately by a factor of 2 during the months from October to April. As the measured values for this period seems to agree well with the model results, we conclude that the proxy in autumn and winter overestimates the H_2SO_4 concentrations considerably and we assume that for this parameter, the model provides a more realistic picture of the sulphuric acid concentrations.

https://doi.org/10.5194/acp-2020-128
Preprint. Discussion started: 22 April 2020

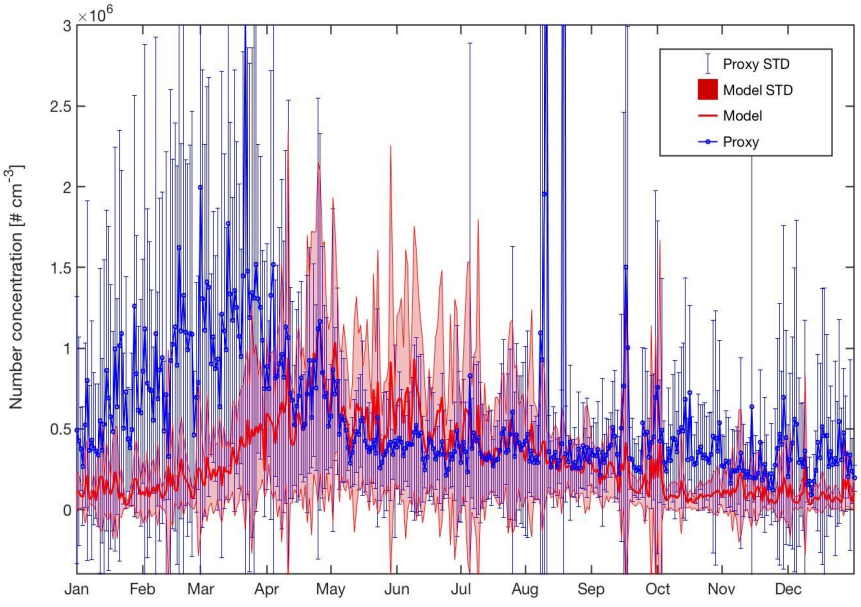

607

608 *Figure 11: Yearly mean daily time series of H_2SO_4 concentrations estimated by SOSAA (Model) and a*
609 *proxy parameterisation (Proxy) for the years 2007-2018 at SMEAR II. Details for the applied proxy*
610 *are provided in the text.*

611

612 The last proxy we want to compare against model results is for the nitrate radical. It is based on a
613 publication by Kontkanen *et al.* (2016). The concentration of NO_3 is calculated based on the following
614 equation:

615 $$[NO_3] = k_{O3+NO2} * [O_3] * [NO_2] * \tau_{NO3} \quad \text{Eq. 3}$$

616 Here k_{O3+NO2} is the temperature-dependent reaction rate coe cient between NO_2 and O_3, which was
617 calculated from a temperature-dependent relation (Atkinson *et al.*, 2004; see Table A1 in Kontkanen *et*
618 *al.*, 2016). τ_{NO3} is the lifetime of NO_3 and a detailed description on the prediction of τ_{NO3} is available in
619 the manuscript by Kontkanen *et al.* (2016).
620 Besides O_3, the nitrate radical is the most important oxidant during nighttime and has an important
621 contribution to BVOC oxidation during nighttime (Mogensen *et al.*, 2015). However, until now, NO_3
622 measurements at SMEAR II are rather limited and most of the existing data achieved during the
623 COPECC-HUMPPA campaign in 2010 (Williams *et al.*, 2011) and the IBAIRN campaign in 2016
624 (Liebmann *et al.*, 2018) were below the LOD.

https://doi.org/10.5194/acp-2020-128
Preprint. Discussion started: 22 April 2020

Atmospheric Chemistry and Physics Discussions

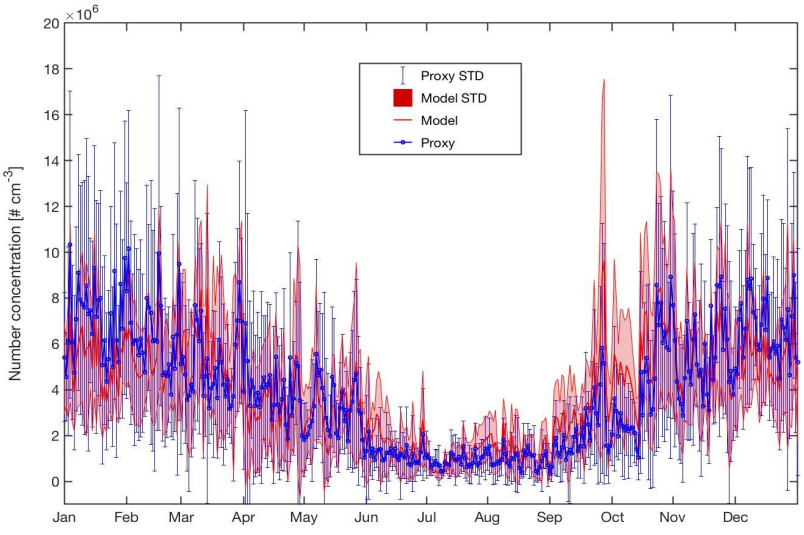

Figure 12: Yearly mean daily time series of NO_3 concentrations estimated by SOSAA (Model) and a proxy parameterization (Proxy) based on reference for the year 2007-2018 at SMEAR II. Details for the applied proxy are provided in the text.

Thus, a robust estimate for NO_3 concentration for the whole year is needed. Previous studies assumed a steady state between the production of NO_3 from the reaction between O_3 and NO_2 and the removal of NO_3 (Kontkanen *et al.*, 2016). This gap could be lled by our study. By applying this approximation, we derived the monthly median NO_3 proxy between 2007-2018. A comparison between the proxy and the model data shows that the long term trend from both methods are in very good agreement (Fig. 12). As those two methods applied here agree very well, it is likely that the predicted values for NO_3 are reliable and could be applied in further studies.

4. Summary and perspectives

In this study we investigated the trends of various measured and modelled meteorological parameters and gaseous compounds at the SMEAR II station in southern Finland for the period 2007-2018. The main focus was on the hydroxyl and the nitrate radical as well as on sulphuric acid, as no long-term measurements of these compounds exist. To validate the SOSAA model, we rstly compared the OH and H_2SO_4 simulations with the intensive measurements from several campaigns. For H_2SO_4 the model underestimates the measured values in spring and summer but reproduces the measurements for the rest of year. OH was only measured during two short campaigns in May 2007 (Kulmala *et al.*, 2011)

https://doi.org/10.5194/acp-2020-128
Preprint. Discussion started: 22 April 2020


Atmospheric Chemistry and Physics Discussions

and August 2010 (Williams *et al.*, 2011). The comparison between observed and modelled OH yielded di erent results in the campaigns of May 2007 and August 2010. In 2007 the model predicted about twice as high values as measured whereas in 2010 the model agreed quite well with measurement, re ecting the existence of an unknown sink(s) in spring and early summer.

The long-term trends (12 years) of the two important oxidants OH and NO_3 was investigated. Our results indicate that the OH concentration is increasing during this period with a rate of +1.56 (-0.8; +3.17) % yr^{-1} for daytime. The main reason is likely decreasing carbon monoxide concentrations (~0.5% yr^{-1}) which is the main sink term for OH. This result was surprising as the monoterpenes, the main biogenic VOC at the SMEAR II increased by about +3.4 (+1.23; +6.02) % yr^{-1} and react strongly with the OH. Therefore, the predicted OH trend shows that the climatic temperature increase (~0.8K in 12 years at SMEAR II) and the followed rise in BVOC emissions is bu ered by a decline of carbon monoxide. In case the current negative trend in CO continues – mostly related to improved combustion techniques – the OH will slightly rise or at least stagnate at the present level which re ects a positive impact on the atmospheric oxidation capacity. Vice versa is the situation for NO_3 showing a nighttime decrease by -3.92 (-6.49; -1.79) % yr^{-1} which is caused by the drop of nitrogen dioxide. As all anthropogenic NO_x emissions in Europe have decreased signi cantly during the last decades (EAA report No 12/2018) and are predicted to decrease further, we expect that the nitrate radical will continue to drop in the future.

Sulphuric acid was investigated as it is one of the most important precursors of new particle formation (NPF). The outcome of our study indicate that the sulphuric acid concentration is decreasing with -5.12 (-11.39; -+0.52) % per year during daytime, which likely is related to the reduction in the emissions of sulphur dioxide in Europe during the last decades (EAA report No 12/2018). In case the negative trend of sulphuric acid (steered by SO_2) will continue in the next decades, it could a ect the amount of NPF events in the boreal region signi cantly. However, whether or not this will have a positive or negative impact on our future climate is currently unclear. In the past, it was typically assumed that NPF events will provide more CCN followed by more cloud droplets, leading to an increased albedo through "brighter" clouds (e.g. Makkonen *et al.*, 2012). In this way, NPF will cool the planet and counteract the e ect of greenhouse gases. However, quite recently Roldin and co-workers' (2019) research result counteracts this assumption by stating that the tiniest particles, under some conditions, are increasing in size at the expense of the larger aerosol particles over the boreal forest – and it is only the latter that have a cooling e ect on the planet. Facing the controversial discussion on this topic in the scienti c community, it is di cult to state whether the decrease of

https://doi.org/10.5194/acp-2020-128
Preprint. Discussion started: 22 April 2020

sulphuric acid should be seen as positive or negative. However, it is certain that H_2SO_4 has decreased in the last decades and, most likely, will continue to drop in the future.

Proxies are commonly applied in case limited amount of parameters are measured and no detailed model simulation are available. We compared concentrations for OH, NO_3 and H_2SO_4 calculated from proxies (Nieminen at al., 2014; Petäjä *et al.*, 2009; Kontkanen *et al.*, 2016) with our model outcomes. Our comparisons showed that the proxies for the OH and H_2SO_4 agree at certain times of the year very well with the model results but also di er signi cantly during other periods. For the nitrate radical, the model and proxy results are in good agreement.

Data availability. All data shown in the gures and tables and additional raw data are available upon request from the corresponding author (P.Z.).

Author contributions. DC and PZ performed the model simulations. DC, M. Boy, M. Baykara and PZ served as the chief authors and editors for the paper. TN and PC suggested and implemented the statistical methods. The scienti c contributions were provided by all co-authors.

Competing interests. The authors declare that they have no con ict of interest.

Special issue statement. This article is part of the special issue “Pan-Eurasian Experiment (PEEX)”. It is not associated with a conference.

Acknowledgements

We acknowledge the support by the Academy of Finland (Center of Excellence in Atmospheric Sciences (grant no. 4100104)) and the computational resources from CSC – IT Center for Science, Finland. Dean Chen acknowledges the China Scholarship Council (201604910541). Putian Zhou acknowledges the University of Helsinki Three Year Grant ("AGES": 2018-2020). Lukas Pichelstorfer acknowledges the Austrian Science Funds (FWF) under grant (J-4241 Schrödinger Programm). Pontus Roldin acknowledges the Swedish Research Council FORMAS (project no. 2014-1445, 2015-749, 2018-01745), the Swedish Research Council VR (project. no. 2019-05006) and the Swedish Strategic Research Program MERGE. Ximeng Qi acknowledges the National Natural Science Foundation of China (41805101).

https://doi.org/10.5194/acp-2020-128
Preprint. Discussion started: 22 April 2020

References

Aaltonen, H., Pumpanen, J., Pihlatie, M., Hakola, H., Hellén, H., Kulmala, L., Vesala, T. and Bäck, J.: Boreal pine forest oor biogenic volatile organic compound emissions peak in early summer and autumn, Agricultural and Forest Meteorology, 151(6), 682–691, doi:10.1016/j.agrformet.2010.12.010, 2011.

Allan, B. J., Plane, J. M. C., Coe, H. and Shillito, J.: Observations of NO_3 concentration pro les in the troposphere, Journal of Geophysical Research Atmospheres, 107(21), doi:10.1029/2002JD002112, 2002.

Asmi, A., Collaud Coen, M., Ogren, J. A., Andrews, E., Sheridan, P., Je erson, A., Weingartner, E., Baltensperger, U., Bukowiecki, N., Lihavainen, H., Kivekäs, N., Asmi, E., Aalto, P. P., Kulmala, M., Wiedensohler, A., Birmili, W., Hamed, A., O'Dowd, C., G Jennings, S., Weller, R., Flentje, H., Fjaeraa, A. M., Fiebig, M., Myhre, C. L., Hallar, A. G., Swietlicki, E., Kristensson, A., and Laj, P.: Aerosol decadal trends – Part 2: In-situ aerosol particle number concentrations at GAW and ACTRIS stations, Atmos. Chem. Phys., 13, 895–916, https://doi.org/10.5194/acp-13-895-2013, 2013.

Atkinson, R. and Arey, J.: Atmospheric Degradation of Volatile Organic Compounds, Chemical Reviews, 103(12), 4605–4638, doi:10.1021/cr0206420, 2003.

Bäck, J., Aalto, J., Henriksson, M., Hakola, H., He, Q. and Boy, M.: Chemodiversity of a Scots pine stand and implications for terpene air concentrations, Biogeosciences, 9(2), 689–702, doi:10.5194/bg-9-689-2012, 2012.

Bey, I., Aumont, B. and Toupance, G.: A modeling study of the nighttime radical chemistry in the lower continental troposphere: 1. Development of a detailed chemical mechanism including nighttime chemistry, Journal of Geophysical Research: Atmospheres, 106(D9), 9959–9990, doi:10.1029/2000JD900347, 2001.

Boleti, E., Hueglin, C. and Takahama, S.: Ozone time scale decomposition and trend assessment from surface observations in Switzerland, Atmospheric Environment, 191, 440–451, doi:10.1016/j.atmosenv.2018.07.039, 2018.

Bonan, G.: Forests and Climate Change: Forcings, Feedbacks, and the Climate Bene ts of Forests, Science, 320 (5882), 1444-1449, DOI: 10.1126/science.1155121, 2008.

Bonn, B., von Kuhlmann, R. and Lawrence, M. G.: High contribution of biogenic hydroperoxides to secondary organic aerosol formation, Geophysical Research Letters, 31(10), L10108, doi:10.1029/2003GL019172, 2004.

https://doi.org/10.5194/acp-2020-128
Preprint. Discussion started: 22 April 2020


Atmospheric Chemistry and Physics Discussions

741 Boy, M., Sogachev, A., Lauros, J., Zhou, L., Guenther, A. and Smolander, S.: SOSA – a new model to
742 simulate the concentrations of organic vapours and sulphuric acid inside the ABL – Part 1: Model
743 description and initial evaluation, Atmospheric Chemistry and Physics, 11(1), 43–51, doi:10.5194/acp-
744 11-43-2011, 2011.
745 Boy, M., Mogensen, D., Smolander, S., Zhou, L., Nieminen, T., Paasonen, P., Plass-Dülmer, C., Sipilä,
746 M., Petäjä, T., Mauldin, L., Berresheim, H. and Kulmala, M.: Oxidation of SO_2 by stabilized Criegee
747 intermediate (sCI) radicals as a crucial source for atmospheric sulfuric acid concentrations,
748 Atmospheric Chemistry and Physics, 13(7), 3865–3879, doi:10.5194/acp-13-3865-2013, 2013.
749 Brown, S. S., Stark, H., Ryerson, T. B., Williams, E. J., Nicks, D. K., Trainer, M., Fehsenfeld, F. C. and
750 Ravishankara, A. R.: Nitrogen oxides in the nocturnal boundary layer: Simultaneous in situ
751 measurements of NO_3, N_2O_5, NO_2, NO, and O_3, Journal of Geophysical Research: Atmospheres,
752 108(D9), 4299, doi:10.1029/2002JD002917, 2003.
753 Carslaw, D. C.: On the changing seasonal cycles and trends of ozone at Mace Head, Ireland,
754 Atmospheric Chemistry and Physics, 5(12), 3441–3450, doi:10.5194/acp-5-3441-2005, 2005.
755 Carslaw, N., Creasey, D. J., Harrison, D., Heard, D. E., Hunter, M. C., Jacobs, P. J., Jenkin, M. E., Lee,
756 J. D., Lewis, A. C., Pilling, M. J., Saunders, S. M. and Seakins, P. W.: OH and HO_2 radical chemistry
757 in a forested region of north-western Greece, Atmospheric Environment, 35(27), 4725–4737,
758 doi:10.1016/S1352-2310(01)00089-9, 2001.
759 Cohen, M. A. and Ryan, P. B.: Observations Less than the Analytical Limit of Detection: A New
760 Approach, JAPCA, 39:3, 328-329, DOI: 10.1080/08940630.1989.10466534, 1989.
761 Crowley, J. N., Schuster, G., Pouvesle, N., Parchatka, U., Fischer, H., Bonn, B., Bingemer, H. and
762 Lelieveld, J.: Nocturnal nitrogen oxides at a rural mountain-site in south-western Germany,
763 Atmospheric Chemistry and Physics, 10(6), 2795–2812, doi:10.5194/acp-10-2795-2010, 2010.
764 Crowley, J. N., Thieser, J., Tang, M. J., Schuster, G., Bozem, H., Beygi, Z. H., Fischer, H., Diesch, J.
765 M., Drewnick, F., Borrmann, S., Song, W., Yassaa, N., Williams, J., Pöhler, D., Platt, U. and Lelieveld,
766 J.: Variable lifetimes and loss mechanisms for NO_3 and N_2O_5 during the DOMINO campaign:
767 Contrasts between marine, urban and continental air, Atmospheric Chemistry and Physics, 11(21),
768 10853–10870, doi:10.5194/acp-11-10853-2011, 2011.
769 Damian, V., Sandu, A., Damian, M., Potra, F. and Carmichael, G. R.: The kinetic preprocessor KPP-a
770 software environment for solving chemical kinetics, Computers & Chemical Engineering, 26(11),
771 1567–1579, doi:10.1016/S0098-1354(02)00128-X, 2002.

https://doi.org/10.5194/acp-2020-128
Preprint. Discussion started: 22 April 2020

772 Dee, D. P., Uppala, S. M., Simmons, A. J., Berrisford, P., Poli, P., Kobayashi, S., Andrae, U.,
773 Balmaseda, M. A., Balsamo, G., Bauer, P., Bechtold, P., Beljaars, A. C. M., van de Berg, L., Bidlot, J.,
774 Bormann, N., Delsol, C., Dragani, R., Fuentes, M., Geer, A. J., Haimberger, L., Healy, S. B., Hersbach,
775 H., Hólm, E. V., Isaksen, L., Kållberg, P., Köhler, M., Matricardi, M., McNally, A. P., Monge-Sanz, B.
776 M., Morcrette, J.-J., Park, B.-K., Peubey, C., de Rosnay, P., Tavolato, C., Thépaut, J.-N. and Vitart, F.:
777 The ERA-Interim reanalysis: con guration and performance of the data assimilation system, Quarterly
778 Journal of the Royal Meteorological Society, 137(656), 553–597, doi:10.1002/qj.828, 2011.
779 Derwent, R. G., Simmonds, P. G., Manning, A. J. and Spain, T. G.: Trends over a 20-year period from
780 1987 to 2007 in surface ozone at the atmospheric research station, Mace Head, Ireland, Atmospheric
781 Environment,41(39),9091–9098,doi:10.1016/j.atmosenv.2007.08.008, 2007.
782 Dlugi, R., Berger, M., Zelger, M., Hofzumahaus, A., Siese, M., Holland, F., Wisthaler, A., Grabmer,
783 W., Hansel, A., Koppmann, R., Kramm, G., Möllmann-Coers, M. and Knaps, A.: Turbulent exchange
784 and segregation of HO_x radicals and volatile organic compounds above a deciduous forest,
785 Atmospheric Chemistry and Physics, 10(13), 6215–6235, doi:10.5194/acp-10-6215-2010, 2010.
786 Elshorbany, Y. F., Kurtenbach, R., Wiesen, P., Lissi, E., Rubio, M., Villena, G., Gramsch, E., Rickard,
787 A. R., Pilling, M. J. and Kle mann, J.: Oxidation capacity of the city air of Santiago, Chile,
788 Atmospheric Chemistry and Physics, 9(6), 2257–2273, doi:10.5194/acp-9-2257-2009, 2009.
789 FAO Global Forest Resources Assessment, Reference: doi:10.1016/j.foreco.2015.06.014, 2015.
790 Feiner, P. A., Brune, W. H., Miller, D. O., Zhang, L., Cohen, R. C., Romer, P. S., Goldstein, A. H.,
791 Keutsch, F. N., Skog, K. M., Wennberg, P. O., Nguyen, T. B., Teng, A. P., DeGouw, J., Koss, A., Wild,
792 R. J., Brown, S. S., Guenther, A., Edgerton, E., Baumann, K. and Fry, J. L.: Testing Atmospheric
793 Oxidation in an Alabama Forest, Journal of the Atmospheric Sciences, 73(12), 4699–4710,
794 doi:10.1175/JAS-D-16-0044.1, 2016.
795 Foken, T.; The energy balance closure problem: an overview, Ecological Applications, 18 (6), 1351-
796 1367, 2008.
797 Ganzeveld, L. N., Lelieveld, J., Dentener, F. J., Krol, M. C. and Roelofs, G. -J.: Atmosphere-biosphere
798 trace gas exchanges simulated with a single-column model, Journal of Geophysical Research,
799 107(D16), 4297, doi:10.1029/2001JD000684, 2002.
800 Gligorovski, S., Strekowski, R., Barbati, S. and Vione, D.: Environmental Implications of Hydroxyl
801 Radicals (•OH), Chemical Reviews, 115(24), 13051–13092, doi:10.1021/cr500310b, 2015.
802 Gordon, H., Kirkby, J., Baltensperger, U., Bianchi, F., Breitenlechner, M., Curtius, J., Dias, A.,
803 Dommen, J., Donahue, N. M., Dunne, E. M., Duplissy, J., Ehrhart, S., Flagan, R. C., Frege, C., Fuchs,

https://doi.org/10.5194/acp-2020-128
Preprint. Discussion started: 22 April 2020

C., Hansel, A., Hoyle, C. R., Kulmala, M., Kürten, A., Lehtipalo, K., Makhmutov, V., Molteni, U., Rissanen, M. P., Stozkhov, Y., Tröstl, J., Tsagkogeorgas, G., Wagner, R., Williamson, C., Wimmer, D., Winkler, P. M., Yan, C. and Carslaw, K. S.: Causes and importance of new particle formation in the present-day and preindustrial atmospheres, Journal of Geophysical Research: Atmospheres, 122, 8739-8760, doi:10.1002/2017JD026844, 2017.

Gratz, L. E., Ja e, D. A. and Hee, J. R.: Causes of increasing ozone and decreasing carbon monoxide in springtime at the Mt. Bachelor Observatory from 2004 to 2013, Atmospheric Environment, 109, 323–330, doi:10.1016/j.atmosenv.2014.05.076, 2015.

Guenther, A., Karl, T., Harley, P., Wiedinmyer, C., Palmer, P. I. and Geron, C.: Estimates of global terrestrial isoprene emissions using MEGAN (Model of Emissions of Gases and Aerosols from Nature), Atmospheric Chemistry and Physics, 6(11), 3181–3210, doi:10.5194/acp-6-3181-2006, 2006.

Hakola, H., Rinne, J. and Laurila, T.: The hydrocarbon emission rates of tea-leafed willow (Salix phylicifolia), silver birch (Betula pendula) and European aspen (Populus tremula), Atmospheric Environment, doi:10.1016/S1352-2310(97)00482-2, 1998.

Hakola, H., Tarvainen, V., Bäck, J., Ranta, H., Bonn, B., Rinne, J. and Kulmala, M.: Seasonal variation of mono- and sesquiterpene emission rates of Scots pine, Biogeosciences, doi:10.5194/bg-3-93-2006, 2006.

Hari, P. and Kulmala, M.: Station for Measuring Ecosystem-Atmosphere Relations (SMEAR II), Boreal Environment Research, 10(5), 315–322, 2005.

Heintz, F., Platt, U., Flentje, H. and Dubois, R.: Long-term observation of nitrate radicals at the Tor Station, Kap Arkona (Rügen), Journal of Geophysical Research: Atmospheres, 101(D17), 22891–22910, doi:10.1029/96JD01549, 1996.

Hellén, H., Praplan, A. P., Tykkä, T., Ylivinkka, I., Vakkari, V., Bäck, J., Petäjä, T., Kulmala, M. and Hakola, H.: Long-term measurements of volatile organic compounds highlight the importance of sesquiterpenes for the atmospheric chemistry of a boreal forest, Atmospheric Chemistry and Physics, 18(19), 13839–13863, doi:10.5194/acp-18-13839-2018, 2018.

Hipel, K.W. and McLeod, A.I.: Time Series Modelling of Water Resources and Environmental Systems, Elsevier, Amsterdam., Volume 45, 1994.

Hussain, M., and Mahmud, I.: pyMannKendall: a python package for non parametric Mann Kendall family of trend tests, Journal of Open Source Software, 4(39), 1556, https://doi.org/10.21105/joss.01556, 2019.

https://doi.org/10.5194/acp-2020-128
Preprint. Discussion started: 22 April 2020

Jacob, D. J. and Winner, D. A.: E ect of climate change on air quality, Atmospheric Environment, 43(1), 51–63, doi.org/10.1016/j.atmosenv.2008.09.051, 2009.

Jenkin, M. E., Saunders, S. M. and Pilling, M. J.: The tropospheric degradation of volatile organic compounds: a protocol for mechanism development, Atmospheric Environment, 31(1), 81–104, doi:10.1016/S1352-2310(96)00105-7, 1997.

Jenkin, M. E., Wyche, K. P., Evans, C. J., Carr, T., Monks, P. S., Alfarra, M. R., Barley, M. H., McFiggans, G. B., Young, J. C. and Rickard, A. R.: Development and chamber evaluation of the MCM v3.2 degradation scheme for β-caryophyllene, Atmospheric Chemistry and Physics, 12(11), 5275–5308, doi:10.5194/acp-12-5275-2012, 2012.

Kanaya, Y., Hofzumahaus, A., Dorn, H.-P., Brauers, T., Fuchs, H., Holland, F., Rohrer, F., Bohn, B., Tillmann, R., Wegener, R., Wahner, A., Kajii, Y., Miyamoto, K., Nishida, S., Watanabe, K., Yoshino, A., Kubistin, D., Martinez, M., Rudolf, M., Harder, H., Berresheim, H., Elste, T., Plass-Dülmer, C., Stange, G., Kle mann, J., Elshorbany, Y. and Schurath, U.: Comparisons of observed and modeled OH and HO_2 concentrations during the ambient measurement period of the HO_xComp eld campaign, Atmospheric Chemistry and Physics, 12(5), 2567–2585, doi:10.5194/acp-12-2567-2012, 2012.

Khalil, M. A. K. and Rasmussen, R. A.: Global decrease in atmospheric carbon monoxide concentration, Nature, 370(6491), 639–641, doi:10.1038/370639a0, 1994.

Kontkanen, J., Paasonen, P., Aalto, J., Bäck, J., Rantala, P., Petäjä, T. and Kulmala, M.: Simple proxies for estimating the concentrations of monoterpenes and their oxidation products at a boreal forest site, Atmospheric Chemistry and Physics, 16(20), 13291–13307, doi:10.5194/acp-16-13291-2016, 2016.

Kubistin, D., Harder, H., Martinez, M., Rudolf, M., Sander, R., Bozem, H., Eerdekens, G., Fischer, H., Gurk, C., Klüpfel, T., Königstedt, R., Parchatka, U., Schiller, C. L., Stickler, A., Taraborrelli, D., Williams, J. and Lelieveld, J.: Hydroxyl radicals in the tropical troposphere over the Suriname rainforest: comparison of measurements with the box model MECCA, Atmospheric Chemistry and Physics, 10(19), 9705–9728, doi:10.5194/acp-10-9705-2010, 2010.

Kulmala, M., Hämeri, K., Aalto, P. P., Mäkelä, J. M., Pirjola, L., Nilsson, E. D., Buzorius, G., Rannik, Ü., Dal Maso, M., Seidl, W., Ho man, T., Janson, R., Hansson, H.-C., Viisanen, Y., Laaksonen, A. and O'dowd, C. D.: Overview of the international project on biogenic aerosol formation in the boreal forest (BIOFOR), Tellus B: Chemical and Physical Meteorology, 53(4), 324–343, doi:10.3402/tellusb.v53i4.16601, 2001.

https://doi.org/10.5194/acp-2020-128
Preprint. Discussion started: 22 April 2020

865 Kulmala, M., Hari, P., Laaksonen, A., Vesala, T. and Viisanen, Y.: Research Unit of Physics,
866 Chemistry and Biology of Atmospheric Composition and Climate Change: Overview of recent results,
867 Boreal Environment Research, 10(6), 459-477, 2005.
868 Kulmala, M., Asmi, A., Lappalainen, H. K., Baltensperger, U., Brenguier, J.-L., Facchini, M. C.,
869 Hansson, H.-C., Hov, Ø., O'Dowd, C. D., Pöschl, U., Wiedensohler, A., Boers, R.,
870 Boucher, O., de Leeuw, G., Denier van der Gon, H. A. C., Feichter, J., Krejci, R., Laj, P., Lihavainen,
871 H., Lohmann, U., McFiggans, G., Mentel, T., Pilinis, C., Riipinen, I., Schulz, M., Stohl, A., Swietlicki,
872 E., Vignati, E., Alves, C., Amann, M., Ammann, M., Arabas, S., Artaxo, P., Baars, H., Beddows, D. C.
873 S., Bergström, R., Beukes, J. P., Bilde, M., Burkhart, J. F., Canonaco, F., Clegg, S. L., Coe, H.,
874 Crumeyrolle, S., D'Anna, B., Decesari, S., Gilardoni, S., Fischer, M., Fjaeraa, A. M.,
875 Fountoukis, C., George, C., Gomes, L., Halloran, P., Hamburger, T., Harrison, R. M., Herrmann, H.,
876 Ho mann, T., Hoose, C., Hu, M., Hyvärinen, A., Hõrrak, U., Iinuma, Y., Iversen, T., Josipovic, M.,
877 Kanakidou, M., Kiendler-Scharr, A., Kirkevåg, A., Kiss, G., Klimont, Z., Kolmonen, P., Komppula,
878 M., Kristjánsson, J.-E., Laakso, L., Laaksonen, A., Labonnote, L., Lanz, V. A., Lehtinen, K. E. J.,
879 Rizzo, L. V., Makkonen, R., Manninen, H. E., McMeeking, G., Merikanto, J., Minikin, A., Mirme, S.,
880 Morgan, W. T., Nemitz, E., O'Donnell, D., Panwar, T. S., Pawlowska, H., Petzold, A.,
881 Pienaar, J. J., Pio, C., Plass-Duelmer, C., Prévôt, A. S. H., Pryor, S., Reddington, C. L., Roberts, G.,
882 Rosenfeld, D., Schwarz, J., Seland, Ø., et al.: General overview: European Integrated project on
883 Aerosol Cloud Climate and Air Quality interactions (EUCAARI) integrating aerosol research from
884 nano to global scales, Atmospheric Chemistry and Physics, 11(24), 13061–13143, doi:10.5194/acp-11-
885 13061-2011, 2011.
886 Laakso, L., Kulmala, M., and Lehtinen, K., E. J.: E ect of condensation rate enhancement factor on 3-
887 nm (diameter) particle formation in binary ion-induced and homogeneous nucleation, Journal of
888 Geophysical Research, 108(D18), 4574, doi:10.1029/2003JD003432, 2003.
889 Liebmann, J., Karu, E., Sobanski, N., Schuladen, J., Ehn, M., Schallhart, S., Quéléver, L., Hellen, H.,
890 Hakola, H., Ho mann, T., Williams, J., Fischer, H., Lelieveld, J. and Crowley, J. N.: Direct
891 measurement of NO_3 radical reactivity in a boreal forest, Atmospheric Chemistry and Physics, 18(5),
892 3799–3815, doi:10.5194/acp-18-3799-2018, 2018.
893 Ma, Z., Xu, J., Quan, W., Zhang, Z., Lin, W. and Xu, X.: Signi cant increase of surface ozone at a
894 rural site, north of eastern China, Atmospheric Chemistry and Physics, 16(6), 3969–3977,
895 doi:10.5194/acp-16-3969-2016, 2016.

https://doi.org/10.5194/acp-2020-128
Preprint. Discussion started: 22 April 2020

Makkonen, R., Asmi, A., Kerminen, V.-M., Boy, M., Arneth, A., Hari, P. and Kulmala, M.: Air pollution control and decreasing new particle formation lead to strong climate warming, Atmos. Chem. Phys., 12, 1515-1524, 2012.

Manning, M. R., Lowe, D. C., Moss, R. C., Bodeker, G. E. and Allan, W.: Short-term variations in the oxidizing power of the atmosphere, Nature, 436(7053), 1001–1004, doi:10.1038/nature03900, 2005.

Mauldin III, R. L., Berndt, T., Sipilä, M., Paasonen, P., Petäjä, T., Kim, S., Kurtén, T., Stratmann, F., Kerminen, V.-M., and Kul- mala, M.: A new atmospherically relevant oxidant, Nature, 488, 193–196, 2012.

Mikkonen, S., Romakkaniemi, S., Smith, J. N., Korhonen, H., Petäjä, T., Plass-Duelmer, C., Boy, M., McMurry, P. H., Lehtinen, K. E. J. J., Joutsensaari, J., Hamed, A., Mauldin, R. L., Birmili, W., Spindler, G., Arnold, F., Kulmala, M., Laaksonen, A., Mauldin III, R. L., Birmili, W., Spindler, G., Arnold, F., Kulmala, M. and Laaksonen, A.: A statistical proxy for sulphuric acid concentration, Atmospheric Chemistry and Physics, 11(21), 11319–11334, doi:10.5194/acp-11-11319-2011, 2011.

Mogensen, D., Gierens, R., Crowley, J. N., Keronen, P., Smolander, S., Sogachev, A., Nölscher, A. C., Zhou, L., Kulmala, M., Tang, M. J., Williams, J. and Boy, M.: Simulations of atmospheric OH, O_3 and NO_3 reactivities within and above the boreal forest, Atmospheric Chemistry and Physics, 15(7), 3909–3932, doi:10.5194/acp-15-3909-2015, 2015.

Montzka, S. A.: New Observational Constraints for Atmospheric Hydroxyl on Global and Hemispheric Scales, Science, 288(5465), 500–503, doi:10.1126/science.288.5465.500, 2000.

Montzka, S. A., Krol, M., Dlugokencky, E., Hall, B., Jöckel, P. and Lelieveld, J.: Small interannual variability of global atmospheric hydroxyl, Science, doi:10.1126/science.1197640, 2011.

Nieminen, T., Manninen, H. E., Sihto, S.-L., Yli-Juuti, T., Mauldin III, R. L., Petäjä, T., Riipinen, I., Kerminen, V.-M. and Kulmala, M.: Connection of Sulfuric Acid to Atmospheric Nucleation in Boreal Forest, Environmental Science & Technology, 43(13), 4715–4721, doi:10.1021/es803152j, 2009.

Nieminen, T., Asmi, A., Aalto, P. P., Keronen, P., Petäjä, T., Kulmala, M., Kerminen, V. M., Nieminen, T. and Dal Maso, M.: Trends in atmospheric new-particle formation: 16 years of observations in a boreal-forest environment, Boreal Environment Research, 2014.

Novelli, P. C.: Reanalysis of tropospheric CO trends: E ects of the 1997–1998 wild res, Journal of Geophysical Research, 108(D15), 4464, doi:10.1029/2002JD003031, 2003.

Ordóñez, C., Brunner, D., Staehelin, J., Hadjinicolaou, P., Pyle, J. A., Jonas, M., Wernli, H., Prévot, A. S. H. and Prévôt, A. S. H.: Strong in uence of lowermost stratospheric ozone on lower tropospheric

https://doi.org/10.5194/acp-2020-128
Preprint. Discussion started: 22 April 2020

background ozone changes over Europe, Geophysical Research Letters, 34(7), L07805, doi:10.1029/2006GL029113, 2007.

Petäjä, T., Mauldin III, R. L., Kosciuch, E., McGrath, J., Nieminen, T., Paasonen, P., Boy, M., Adamov, A., Kotiaho, T., Kulmala, M., Mauldin, R. L., Kosciuch, E., McGrath, J., Nieminen, T., Paasonen, P., Boy, M., Adamov, A., Kotiaho, T. and Kulmala, M.: Sulfuric acid and OH concentrations in a boreal forest site, Atmospheric Chemistry and Physics, 9(19), 7435–7448, doi:10.5194/acp-9-7435-2009, 2009.

Petrenko, V. V., Martinerie, P., Novelli, P., Etheridge, D. M., Levin, I., Wang, Z., Blunier, T., Chappellaz, J., Kaiser, J., Lang, P., Steele, L. P., Hammer, S., Mak, J., Langenfelds, R. L., Schwander, J., Severinghaus, J. P., Witrant, E., Petron, G., Battle, M. O., Forster, G., Sturges, W. T., Lamarque, J.-F., Ste en, K. and White, J. W. C.: A 60 yr record of atmospheric carbon monoxide reconstructed from Greenland rn air, Atmospheric Chemistry and Physics, 13(15), 7567–7585, doi:10.5194/acp-13-7567-2013, 2013.

Pirjola, L., Kulmala, M., Bischo , A., Wilck, M. and Stratmann, F.: E ects of aerosol dynamics on the formation of sulphuric acid aerosols, Journal of Aerosol Science, 29, S825–S826, doi:10.1016/S0021-8502(98)90595-X, 1998.

Praplan, A. P., Tykkä, T., Chen, D., Boy, M., Taipale, D., Vakkari, V., Zhou, P., Petäjä, T. and Hellén, H.: Long-term total OH reactivity measurements in a boreal forest, Atmospheric Chemistry and Physics, 19(23), 14431–14453, doi:10.5194/acp-19-14431-2019, 2019.

Prinn, R. G., Huang, J., Weiss, R. F., Cunnold, D. M., Fraser, P. J., Simmonds, P. G., McCulloch, A., Harth, C., Salameh, P., O'Doherty, S., Wang, R. H. J., Porter, L. and Miller, B. R.: Evidence for substantial variations of atmospheric hydroxyl radicals in the past two decades, Science, 292(5523), 1882–1888, doi:10.1126/science.1058673, 2001.

Regelin, E., Harder, H., Martinez, M., Kubistin, D., Tatum Ernest, C., Bozem, H., Klippel, T., Hosaynali-Beygi, Z., Fischer, H., Sander, R., Jöckel, P., Königstedt, R. and Lelieveld, J.: HO_x measurements in the summertime upper troposphere over Europe: a comparison of observations to a box model and a 3-D model, Atmospheric Chemistry and Physics, 13(21), 10703–10720, doi:10.5194/acp-13-10703-2013, 2013.

Ren, X., Brune, W. H., Cantrell, C. A., Edwards, G. D., Shirley, T., Metcalf, A. R. and Lesher, R. L.: Hydroxyl and Peroxy Radical Chemistry in a Rural Area of Central Pennsylvania: Observations and Model Comparisons, Journal of Atmospheric Chemistry, 52(3), 231–257, doi:10.1007/s10874-005-3651-7, 2005.

https://doi.org/10.5194/acp-2020-128
Preprint. Discussion started: 22 April 2020


Atmospheric Chemistry and Physics Discussions

959 Riccobono, F., Schobesberger, S., Scott, C. E., Dommen, J., Ortega, I. K., Rondo, L., Almeida, J.,
960 Amorim, A., Bianchi, F., Breitenlechner, M., David, A., Downard, A., Dunne, E. M., Duplissy, J.,
961 Ehrhart, S., Flagan, R. C., Franchin, A., Hansel, A., Junninen, H., Kajos, M., Keskinen, H., Kupc, A.,
962 Kurten, A., Kvashin, A. N., Laaksonen, A., Lehtipalo, K., Makhmutov, V., Mathot, S., Nieminen, T.,
963 Onnela, A., Petaja, T., Praplan, A. P., Santos, F. D., Schallhart, S., Seinfeld, J. H., Sipila, M.,
964 Spracklen, D. V., Stozhkov, Y., Stratmann, F., Tome, A., Tsagkogeorgas, G., Vaattovaara, P., Viisanen,
965 Y., Vrtala, A., Wagner, P. E., Weingartner, E., Wex, H., Wimmer, D., Carslaw, K. S., Curtius, J.,
966 Donahue, N. M., Kirkby, J., Kulmala, M., Worsnop, D. R. and Baltensperger, U.: Oxidation Products
967 of Biogenic Emissions Contribute to Nucleation of Atmospheric Particles, Science, 344(6185), 717–
968 721, doi:10.1126/science.1243527, 2014.
969 Rinne, J., Bäck, J. and Hakola, H.: Biogenic volatile organic compound emissions from the Eurasian
970 taiga: Current knowledge and future directions, Boreal Environment Research, 14(4), 807–826, 2009.
971 Rohrer, F. and Berresheim, H.: Strong correlation between levels of tropospheric hydroxyl radicals and
972 solar ultraviolet radiation, Nature, 442(7099), 184–187, doi:10.1038/nature04924, 2006.
973 Roldin, P., Swietlicki, E., Massling, A., Kristensson, A., Löndahl, J., Eriksson, A., Pagels, J. and
974 Gustafsson, S.: Aerosol ageing in an urban plume – implication for climate, Atmospheric Chemistry
975 and Physics, 11(12), 5897–5915, doi:10.5194/acp-11-5897-2011, 2011.
976 Roldin, P., Ehn, M., Kurtén, T., Olenius, T., Rissanen, M. P., Sarnela, N., Elm, J., Rantala, P., Hao, L.,
977 Hyttinen, N., Heikkinen, L., Worsnop, D. R., Pichelstorfer, L., Xavier, C., Clusius, P., Öström, E.,
978 Petäjä, T., Kulmala, M., Vehkamäki, H., Virtanen, A., Riipinen, I. and Boy, M.: The role of highly
979 oxygenated organic molecules in the Boreal aerosol-cloud-climate system, Nature Communications,
980 10(1), 4370, doi:10.1038/s41467-019-12338-8, 2019.
981 Räisänen, J.: E ect of atmospheric circulation on recent temperature changes in Finland, Climate
982 Dynamics, 53, 5676-5687, https://link.springer.com/article/10.1007/s00382-019-04890-2, 2019
983 Salisbury, G., Rickard, A. R., Monks, P. S., Allan, B. J., Bauguitte, S., Penkett, S. A., Carslaw, N.,
984 Lewis, A. C., Creasey, D. J., Heard, D. E., Jacobs, P. J. and Lee, J. D.: Production of peroxy radicals at
985 night via reactions of ozone and the nitrate radical in the marine boundary layer, Journal of
986 Geophysical Research: Atmospheres, 106(D12), 12669–12687, doi:10.1029/2000JD900754, 2001.
987 Saunders, S. M., Jenkin, M. E., Derwent, R. G. and Pilling, M. J.: Protocol for the development of the
988 Master Chemical Mechanism, MCM v3 (Part A): tropospheric degradation of non-aromatic volatile
989 organic compounds, Atmospheric Chemistry and Physics, 3(1), 161–180, doi:10.5194/acp-3-161-
990 2003, 2003.

https://doi.org/10.5194/acp-2020-128
Preprint. Discussion started: 22 April 2020

991 Schultz, M. G., Akimoto, H., Bottenheim, J., Buchmann, B., Galbally, I. E., Gilge, S., Helmig, D.,
992 Koide, H., Lewis, A. C., Novelli, P. C., Plass-Dülmer, C., Ryerson, T. B., Steinbacher, M.,
993 Steinbrecher, R., Tarasova, O., Tørseth, K., Thouret, V. and Zellweger, C.: The Global Atmosphere
994 Watch reactive gases measurement network, Elem Sci Anth, 3, doi:10.12952/journal.elementa.000067,
995 2015.
996 Smolander, S., He, Q., Mogensen, D., Zhou, L., Bäck, J., Ruuskanen, T., Noe, S., Guenther, A.,
997 Aaltonen, H., Kulmala, M. and Boy, M.: Comparing three vegetation monoterpene emission models to
998 measured gas concentrations with a model of meteorology, air chemistry and chemical transport,
999 Biogeosciences, 11(19), 5425–5443, doi:10.5194/bg-11-5425-2014, 2014.
1000 Sobanski, N., Tang, M. J., Thieser, J., Schuster, G., Pöhler, D., Fischer, H., Song, W., Sauvage, C.,
1001 Williams, J., Fachinger, J., Berkes, F., Hoor, P., Platt, U., Lelieveld, J. and Crowley, J. N.: Chemical
1002 and meteorological in uences on the lifetime of NO3 at a semi-rural mountain site during PARADE,
1003 Atmospheric Chemistry and Physics, 16(8), 4867–4883, doi:10.5194/acp-16-4867-2016, 2016.
1004 Sogachev, A. and Panferov, O.: Modi cation of Two-Equation Models to Account for Plant Drag,
1005 Boundary-Layer Meteorology, 121(2), 229–266, doi:10.1007/s10546-006-9073-5, 2006.
1006 Sogachev, A., Menzhulin, G. V., Heimann, M. and Lloyd, J.: A simple three-dimensional canopy -
1007 planetary boundary layer simulation model for scalar concentrations and uxes, Tellus B, 54(5), 784–
1008 819, doi:10.1034/j.1600-0889.2002.201353.x, 2002.
1009 Sogachev, A., Panferov, O., Gravenhorst, G. and Vesala, T.: Numerical analysis of ux footprints for
1010 di erent landscapes, Theoretical and Applied Climatology, 80(2-4), 169–185, doi:10.1007/s00704-
1011 004-0098-8, 2005.
1012 Stone, D., Evans, M. J., Walker, H., Ingham, T., Vaughan, S., Ouyang, B., Kennedy, O. J., McLeod, M.
1013 W., Jones, R. L., Hopkins, J., Punjabi, S., Lidster, R., Hamilton, J. F., Lee, J. D., Lewis, A. C.,
1014 Carpenter, L. J., Forster, G., Oram, D. E., Reeves, C. E., Bauguitte, S., Morgan, W., Coe, H., Aru o,
1015 E., Dari-Salisburgo, C., Giammaria, F., Di Carlo, P. and Heard, D. E.: Radical chemistry at night:
1016 Comparisons between observed and modelled HOx, NO3 and N2O5 during the RONOCO project,
1017 Atmospheric Chemistry and Physics, 14(3), 1299–1321, doi:10.5194/acp-14-1299-2014, 2014.
1018 Tan, D., Faloona, I., Simpas, J. B., Brune, W., Shepson, P. B., Couch, T. L., Sumner, A. L., Carroll, M.
1019 A., Thornberry, T., Apel, E., Riemer, D. and Stockwell, W.: HO_x budgets in a deciduous forest: Results
1020 from the PROPHET summer 1998 campaign, Journal of Geophysical Research: Atmospheres,
1021 106(D20), 24407–24427, doi:10.1029/2001JD900016, 2001.

https://doi.org/10.5194/acp-2020-128
Preprint. Discussion started: 22 April 2020


Atmospheric Chemistry and Physics Discussions

1022 Tan, Z., Lu, K., Jiang, M., Su, R., Wang, H., Lou, S., Fu, Q., Zhai, C., Tan, Q., Yue, D., Chen, D.,
1023 Wang, Z., Xie, S., Zeng, L. and Zhang, Y.: Daytime atmospheric oxidation capacity in four Chinese
1024 megacities during the photochemically polluted season: a case study based on box model simulation,
1025 Atmospheric Chemistry and Physics, 19(6), 3493–3513, doi:10.5194/acp-19-3493-2019, 2019.
1026 Toon, O. B., McKay, C. P., Ackerman, T. P. and Santhanam, K.: Rapid calculation of radiative heating
1027 rates and photodissociation rates in inhomogeneous multiple scattering atmospheres, Journal of
1028 Geophysical Research, 94(D13), 16287, doi:10.1029/jd094id13p16287, 1989.
1029 Turner, A. J., Frankenberg, C., Wennberg, P. O. and Jacob, D. J.: Ambiguity in the causes for decadal
1030 trends in atmospheric methane and hydroxyl, Proceedings of the National Academy of Sciences of the
1031 United States of America, 114(21), 5367–5372, doi:10.1073/pnas.1616020114, 2017.
1032 Volkamer, R., Sheehy, P., Molina, L. T. and Molina, M. J.: Oxidative capacity of the Mexico City
1033 atmosphere – Part 1: A radical source perspective, Atmospheric Chemistry and Physics, 10(14), 6969–
1034 6991, doi:10.5194/acp-10-6969-2010, 2010.
1035 Wang, Z., Chappellaz, J., Martinerie, P., Park, K., Petrenko, V., Witrant, E., Emmons, L. K., Blunier,
1036 T., Brenninkmeijer, C. A. M. and Mak, J. E.: The isotopic record of Northern Hemisphere atmospheric
1037 carbon monoxide since 1950: Implications for the CO budget, Atmospheric Chemistry and Physics,
1038 12(10), 4365-4377, doi:10.5194/acp-12-4365-2012, 2012.
1039 Welz, O., Savee, J. D., Osborn, D. L., Vasu, S. S., Percival, C. J., Shallcross, D. E., and Taatjes, C. A.:
1040 Direct kinetic measure- ments of Criegee Intermediate (CH2OO) formed by reaction of CH2I with O2,
1041 Science, 335, 204–207, 2012.
1042 Wilks, D. S.: Resampling Hypothesis Tests for Autocorrelated Fields, Journal of Climate, 10(1), 65–
1043 82, doi:10.1175/1520-0442, 1997.
1044 Williams, J., Crowley, J., Fischer, H., Harder, H., Martinez, M., Petäjä, T., Rinne, J., Bäck, J., Boy, M.,
1045 Dal Maso, M., Hakala, J., Kajos, M., Keronen, P., Rantala, P., Aalto, J., Aaltonen, H., Paatero, J.,
1046 Vesala, T., Hakola, H., Levula, J., Pohja, T., Herrmann, F., Auld, J., Mesarchaki, E., Song, W., Yassaa,
1047 N., Nölscher, A., Johnson, A. M., Custer, T., Sinha, V., Thieser, J., Pouvesle, N., Taraborrelli, D., Tang,
1048 M. J., Bozem, H., Hosaynali-Beygi, Z., Axinte, R., Oswald, R., Novelli, A., Kubistin, D., Hens, K.,
1049 Javed, U., Trawny, K., Breitenberger, C., Hidalgo, P. J., Ebben, C. J., Geiger, F. M., Corrigan, A. L.,
1050 Russell, L. M., Ouwersloot, H. G., de Arellano, J., Ganzeveld, L., Vogel, A., Beck, M., Bayerle, A.,
1051 Kampf, C. J., Bertelmann, M., Köllner, F., Ho mann, T., Valverde, J., González, D., Riekkola, M.-L.,
1052 Kulmala, M. and Lelieveld, J.: The summertime Boreal forest eld measurement intensive (HUMPPA-

https://doi.org/10.5194/acp-2020-128
Preprint. Discussion started: 22 April 2020

Atmospheric Chemistry and Physics Discussions

1053 COPEC-2010): an overview of meteorological and chemical in uences, Atmospheric Chemistry and
1054 Physics, 11(20), 10599–10618, doi:10.5194/acp-11-10599-2011, 2011.
1055 Wilson, R. C., Fleming, Z. L., Monks, P. S., Clain, G., Henne, S., Konovalov, I. B., Szopa, S. and
1056 Menut, L.: Have primary emission reduction measures reduced ozone across Europe? An analysis of
1057 European rural background ozone trends 1996–2005, Atmospheric Chemistry and Physics, 12(1), 437–
1058 454, doi:10.5194/acp-12-437-2012, 2012.
1059 Yan, Y., Pozzer, A., Ojha, N., Lin, J. and Lelieveld, J.: Analysis of European ozone trends in the period
1060 1995–2014, Atmospheric Chemistry and Physics, 18(8), 5589–5605, doi:18/5589/2018/, 2018.
1061 Zhang, C., Li, S., Luo, F. and Huang, Z.: The global warming hiatus has faded away: An analysis of
1062 2014–2016 global surface air temperatures, International Journal of Climatology, 39(12), 4853-4868,
1063 doi:10.1002/joc.6114, 2019.
1064 Zhou, L., Nieminen, T., Mogensen, D., Smolander, S., Rusanen, A., Kulmala, M. and Boy, M.:
1065 SOSAA — a new model to simulate the concentrations of organic vapours, sulphuric acid and aerosols
1066 inside the ABL — Part 2: Aerosol dynamics and one case study at a boreal forest site, Boreal
1067 Environment Research, 19(suppl. B), 237–256 [online] Available from:
1068 https://helda.helsinki. /handle/10138/165201, 2014.
1069 Zhou, P., Ganzeveld, L., Taipale, D., Rannik, Ü., Rantala, P., Petteri Rissanen, M., Chen, D. and Boy,
1070 M.: Boreal forest BVOC exchange: Emissions versus in-canopy sinks, Atmospheric Chemistry and
1071 Physics, 17(23), 14309–14332, doi:10.5194/acp-17-14309-2017, 2017a.
1072 Zhou, P., Ganzeveld, L., Rannik, Ü., Zhou, L., Gierens, R., Taipale, D., Mammarella, I. and Boy, M.:
1073 Simulating ozone dry deposition at a boreal forest with a multi-layer canopy deposition model,
1074 Atmospheric Chemistry and Physics, 17(2), 1361–1379, doi:10.5194/acp-17-1361-2017, 2017b.